Forest Systems
28 (1), e00R1, 33 pages (2019)
eISSN: 2171-9292
https://doi.org/10.5424/fs/2019281-14221
Instituto Nacional de Investigación y Tecnología Agraria y Alimentaria, O.A, M.P. (INIA)

REVIEW ARTICLE

OPEN ACCESS

Remote sensing for the Spanish forests in the 21st century: a review of advances, needs, and opportunities

Cristina Gómez*[1,2], Pablo Alejandro[3], Txomin Hermosilla[4,5], Fernando Montes[1], Cristina Pascual[6], Luis Ángel Ruiz[7], Flor Álvarez-Taboada[8], Mihai A. Tanase[9, 10] and Rubén Valbuena[11, 12, 13]

[1]INIA. Forest Research Centre. Department of Forest Dynamics and Management. Ctra. La Coruña km 7.5 28040 Madrid, Spain. [2]Department of Geography and Environment, School of Geoscience, University of Aberdeen, Aberdeen AB24 3UE, Scotland, UK. [3]Quasar Science Resources, Ctra. La Coruña km 22.3, Las Rozas, 28232 Madrid, Spain. [4]Canadian Forest Service (Pacific Forestry Centre), Natural Resources Canada, 506 West Burnside Road, Victoria, British Columbia, V8Z 1M5, Canada. [5]Integrated Remote Sensing Studio, Department of Forest Resources Management, University of British Columbia, 2424 Main Mall, Vancouver, BC, V6T 1Z4, Canada. [6]Sustainable Environmental Management Group (SILVANET), Department of Forest and Environmental Engineering and Management. Universidad Politécnica de Madrid, Ciudad Universitaria s/n, 28040 Madrid, Spain. [7]Geo-Environmental Cartography and Remote Sensing Group, Department of Cartographic Engineering, Geodesy and Photogrammetry, Universitat Politècnica de València, Camí de Vera s/n, 46022 Valencia, Spain. [8]Geomatics and Cartography Engineering Group (GEOINCA), Department of Cartographic Engineering, Geodesy and Photogrammetry, Universidad de León, Campus de Ponferrada, Avda. Astorga s/n, 24401 Ponferrada, León, Spain. [9]Department of Geology, Geography and Environment, University of Alcalá, C. Colegios 2, Alcalá de Henares 28801, Spain. [10]National Institute for Research and Development in Forestry, Bd. Eroilor 128, Ilfov, Romania. [11]University of Cambridge, Department of Plant Sciences, Forest Ecology and Conservation, Downing Street, CB2 3EA Cambridge, UK. [12]University of Cambridge, Department of Plant Sciences, Forest Ecology and Conservation, Downing Street, CB2 3EA Cambridge, UK. [12]University of Eastern Finland, Faculty of Forest Sciences, PO Box 111, Joensuu, Finland. [13]Bangor University, School of Natural Sciences, LL57 2DGA Bangor, UK.

Abstract

Forest ecosystems provide a host of services and societal benefits, including carbon storage, habitat for fauna, recreation, and provision of wood or non-wood products. In a context of complex demands on forest resources, identifying priorities for biodiversity and carbon budgets require accurate tools with sufficient temporal frequency. Moreover, understanding long term forest dynamics is necessary for sustainable planning and management. Remote sensing (RS) is a powerful means for analysis, synthesis, and report, providing insights and contributing to inform decisions upon forest ecosystems. In this communication we review current applications of RS techniques in Spanish forests, examining possible trends, needs, and opportunities offered by RS in a forestry context. Currently, wall-to-wall optical and LiDAR data are extensively used for a wide range of applications—many times in combination—whilst radar or hyperspectral data are rarely used in the analysis of Spanish forests. Unmanned Aerial Vehicles (UAVs) carrying visible and infrared sensors are gaining ground in acquisition of data locally and at small scale, particularly for health assessments. Forest fire identification and characterization are prevalent applications at the landscape scale, whereas structural assessments are the most widespread analyses carried out at limited extents. Unparalleled opportunities are offered by the availability of diverse RS data like those provided by the European Copernicus programme and recent satellite LiDAR launches, processing capacity, and synergies with other ancillary sources to produce information of our forests. Overall, we live in times of unprecedented opportunities for monitoring forest ecosystems with a growing support from RS technologies.

Additional keywords: optical, radar, LiDAR, UAV, forest structure, forest fire, forest health.

Authors' contributions: CG conceived the work; all authors have contributed to drafting the manuscript and critically revising the intellectual content.

Citation: Gómez, C.; Alejandro, P.; Hermosilla, T.; Montes, F.; Pascual. C.; Ruiz, L-A.; Álvarez-Taboada, F.; Tanase, M-A.; Valbuena, R. (2019). Remote sensing for the Spanish forests in the 21st century: a review of advances, needs, and opportunities. Forest Systems, Volume 28, Issue 1, eR001. https://doi.org/10.5424/fs/2019281-14221

Received: 6 Nov 2018. **Accepted:** 22 Feb 2019.

Funding: Part of this work was funded by the Spanish Ministry of Science, Innovation and University through the project AGL2016-76769-C2-1-R "Influence of natural disturbance regimes and management on forests dynamics, structure and carbon balance (FORESTCHANGE)".

Competing interests: The authors have declared that no competing interests exist.

Correspondence should be addressed to Cristina Gómez: gomez.cristina@inia.es

Introduction

Forests and other woodlands cover 27.7 million hectares of the Spanish land (MAPAMA, 2011; INE, 2017), and provide important services such as carbon storage, habitat for fauna, wood and non-wood products, as well as societal benefits like education, recreation, and conservation (Montero & Serrada,

2013). Spanish forests are variable in composition, comprising more than 150 tree species and have an overall complex structure (Alberdi *et al.*, 2017). Forests in mountain areas are generally dominated by *Pinus, Quercus, Fagus, Abies* or *Betula* species. Many of these forests are structurally complex and considered natural. Natural forests coexist with very homogeneous coniferous reforestations from the middle 20th century in the Mediterranean region and with fast growing plantations of *Pinus* and *Eucalyptus* in the Atlantic region. In the plains open woodlands (named *dehesas*) and dense forests (often as coppices) dominated by *Quercus* and *Fraxinus* are spread over the Mediterranean area, along with pinewoods managed for production of timber, fruit and resin, and productive plantations of *Populus* and *Eucalyptus* (MAPAMA, 2011). Forests may be difficult to access, especially in the mountains, making field work inconvenient and giving added value to remote sensing (RS) technologies. Under a multi-functional and sustainable forest management paradigm (Cubbage *et al.*, 2007) monitoring forests poses specific reporting requirements. A traditional field-sampling-based long rotation (*e.g.*, 10 years) inventory of wood products followed by statistical generalization does not cover current information needs for multipurpose sustainable management, which requires more frequent data acquisition to fulfil national and international reporting obligations, especially where fast-growing species are planted (Diaz-Balteiro & Romero, 2008). Carbon and biodiversity reports demand frequent, specific, and detailed characterizations based on systematically acquired data that enable comparable and harmonized information as required by global policies. Moreover, understanding forest dynamics and drivers of change at various spatio-temporal scale is essential for preservation and management in a context of rapid change, and requires up to date data to be regularly acquired.

Remote sensing technology provides an exceptional source of data acquired with overview perspective, and powerful tools for monitoring forest dynamics and the drivers of change. RS provides data at a variety of spectral, spatial, and temporal resolutions enabling modelling forest condition and change under different scenarios. Forestry applications have benefited from RS data since Earth observations were available in the early 1970s (Cohen & Goward, 2004). Applications have become more detailed and specific with the improvement of data quality, storage capacity, and analysis techniques, and also as result of the information needs imposed by society, going from simple characterization to complex measure and modelling. As forest management policies intensify preservation, and international agreements on forest monitoring begin to include forest degradation (Kissinger *et al.*, 2012) there are greater demands on RS to provide a range of detection capabilities (Cohen *et al.*, 2018). Applying RS methods in Mediterranean forests may pose a different set of challenges to those found in temperate, boreal, or tropical forests, related to the low canopy density and the presence of shrubs and understory vegetation in some forest types. Likewise, RS application in the Spanish Atlantic region requires attention to the complexity of the landscape, which results from fire regimes and impacts the forest structure.

Current international Earth Observation programmes such as the European Copernicus with the Sentinel satellites, or the USA Landsat and MODIS provide huge amounts of data accessible online (Table 1), including their processing standards to facilitate use. Although data access policies are variable, there is an increasing trend towards data free of economic cost to all users (*e.g.*, Sentinel, Landsat), and some programs facilitate the use for research with reduced costs (*e.g.*, the Advanced Land Observation Satellite, Phased Array type L-band Synthetic Aperture Radar—ALOS PALSAR) (Table 1). The frequency of available and useable observations depends on mission characteristics, cloud regime (for optical data), and sometimes historical management (Wulder *et al.*, 2016). MODIS acquires daily observations with various spatial resolutions (250-1000 m), whereas Landsat OLI/ETM+ and the Sentinel-2A/B MSI observe the entire Earth with 8 and 5-days intervals respectively (Li & Roy, 2017) providing optical data of medium to high spatial resolution (10-60 m). Sentinel-2 and Landsat-OLI optical sensors are highly compatible and constitute a virtual satellite constellation (Wulder *et al.*, 2015; Claverie *et al.*, 2018). In Spain, the National Territory Observation Program (Plan Nacional de Observación del Territorio, PNOT) (Arozarena *et al.*, 2006) which coordinates the acquisition and sharing of national geographic information, encompases SIOSE (Sistema de Información sobre Ocupación del Suelo en España), PNT (Plan Nacional de Teledetección), and PNOA (Plan Nacional de Ortofotografía Aérea). PNOT supplies RS data covering the entire country, including aerial multispectral orthophotography updated every 3 years (http://pnoa.ign.es/) and airborne LiDAR coverage intended to be updated every 6 years. The first LiDAR acquisition (density of 0.5 point × m^{-2}) was acquired between 2009 and 2015. A second LiDAR acquisition with variable pulse density dependent on regional government co-funding (0.5-14 pulse × m^{-2}) is being acquired since 2015 and expected to be completed by 2020, promising important opportunities to assist forest monitoring.

Table 1. Examples of currently operational satellites providing data applicable in forest monitoring.

Satellite (Sensor)	Data type	Revisit (day)	Cost policy	Reference
Landsat (ETM+, OLI)	Optical	16 (8)*	Free	https://landsat.usgs.gov/about-landsat
Sentinel-1 (SAR)	Radar	12 (6)**	Free	https://earth.esa.int/web/sentinel/user-guides/sentinel-1-sar
Sentinel-2 (MSI)	Optical	10 (5)**	Free	https://earth.esa.int/web/sentinel/user-guides/sentinel-2-msi
Terra and Aqua (MODIS)	Optical	2 (1)**	Free	https://modis.gsfc.nasa.gov/about/specifications.php
ALOS-2 (PALSAR)	Radar	14	Under research licence	http://global.jaxa.jp/projects/sat/alos2/index.html
Radarsat-2	Radar	24	Under research licence	https://mdacorporation.com/geospatial/international/satellites/RADARSAT-2
TanDEM-X	Radar	11	Under research licence	https://www.dlr.de/dlr/en/desktopdefault.aspx/tab-id-10378/566_read-426/#/gallery/345
WorldView- 2, 3, 4	Optical	1	Commercial	https://www.satimagingcorp.com/satellite-sensors
RapidEye	Optical	2.1-8.3	Commercial	https://www.satimagingcorp.com/satellite-sensors

*Note. Landsat 7 ETM+ and Landsat 8 OLI constitute a virtually dual program with highly compatible data.**Note. Sentinel-1(A/B) and Sentinel-2(A/B) are dual satellite missions with opposed orbits: Sentinel-1 satellites have a 12-day repetition interval and together provide a 6-day repetition, while Sentinel-2 satellites have a 10-day interval (together 5-day repetition). Terra and Aqua also compose a dual satellite system carrying the MODIS instrument: each satellite has a 2-day repetition interval and together they provide daily repetition interval.

This communication reviews the RS technologies employed to monitor the Spanish forest ecosystems during the last decades, and identifies opportunities offered by the currently available data and analysis techniques. In the next section an overview of RS technologies is presented, followed by a review section of RS applications in Spanish forests. We then wrap-up with a synthesis of the current needs and opportunities offered by RS to monitor the Spanish forests.

Remote sensing techniques

Remote Sensing involves a range of technologies including acquisition of data from a certain distance and their analysis. The platform type (*i.e.*, satellite, aircraft, unmanned aerial vehicle—UAV) and on-board sensor (*i.e.*, optical, thermal, LiDAR, radar) determines the characteristics of the data acquired, which in turn influences the potential applications. Sensors may be active or passive, according to whether they emit energy toward the target object, or just detect sun radiation reaching the sensor. Passive sensors (*e.g.*, optical, hyperspectral) take advantage of the sun energy, whilst active sensors (*e.g.*, radar, LiDAR) beam their own energy pulses. RS synergically combines with Geographic Information Systems (GIS) and machine learning for spatial data analysis and modelling (Figure 1). Herein we provide an overview of RS techniques commonly used in forest applications in Spain, grouped by the characteristics of the data acquired.

Aerial photogrammetry

Aerial photographs have been used as base for developing forest maps and resource inventories

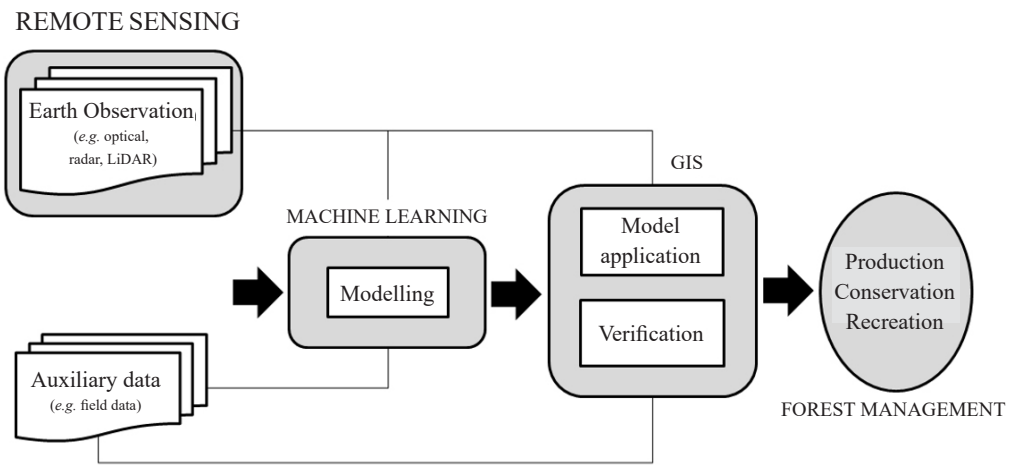

Figure 1. Example of a typical flowchart for application of RS technology in forest monitoring.

since the 1930s (Moessner, 1953) and these images are frequently used as reference or validation data. Photogrammetric techniques for analysis are well established, and interpretation is also intuitive. A very high spatial resolution (0.1-0.25 m) is the strongest trait of aerial photography, and when accurately geo-referenced it facilitates precise identification of objects on the ground. Its low temporal repetition and limited spatial coverage—both related to high cost of acquisition—limit a more generalized use of aerial photography. Tree top displacement in overlapping photo acquisitions and tree shadows have traditionally been used for estimation of tree heights using photogrammetry. Nowadays, digital aerial photography (DAP) provides a source of 3D information enabled by recent improvements in sensor technology and image matching algorithms (Leberl *et al.*, 2010) like *Structure from Motion* (SfM) and *Multiview-Stereo* (MVS). These image matching algorithms facilitate producing point clouds to reconstruct forest three dimensional structure in near real time (Smith *et al.*, 2016). Radiometric data captured by DAP can be employed for stand delineation and characterization, as well as for identification of forest species (Packalén & Maltamo, 2006; Packalén *et al.*, 2009). Point clouds derived from DAP provide limited information about vertical distribution of vegetation within the canopy, and they lack capacity to provide information about the position of the ground (Lisein *et al.*, 2013). Alternatively, DAP can be efficiently combined with LiDAR (see below) (Packalén *et al.*, 2009; Valbuena *et al.*, 2011) for measurement of vegetation heights whilst informing spectral features (Manzanera *et al.*, 2016), posing new opportunities for improving the certainty of forest estimations (Valbuena *et al.*, 2013a; 2017a).

Satellite optical remote sensing

Optical remote sensing is the most commonly used RS technique for monitoring forests (Wulder, 1998), due to an intuitive interpretation of the visual spectrum and to the wide range of spatial (*i.e.*, from a few cm to some km) and temporal resolutions offered. Optical sensors are passive sensors that record values of the returned sun radiation from targets on the Earth, enabling relative comparison of spectral response in space (single date observations) and time (multi-temporal observations). Strong relationships are found between forest reflectance at different wavelengths—visible (0.4-0.7 μm), near-infrared (0.7-1.5 μm), and shortwave infrared (1.5-3.0 μm)—and forest parameters, thus enabling the construction of direct models (*e.g.*, biomass and species diversity), as well as identification of landscape disturbances and recovery (White *et al.*, 2017) and drivers of change over time (Kennedy *et al.*, 2015; Oeser *et al.*, 2017). When related to biomass and other forest parameters, optical sensors are limited by the saturation of spectral values (Turner *et al.*, 1999; Duncanson *et al.*, 2010), that is, given a threshold value of *e.g.*, biomass, reflectance response does not change.

Numerous satellite missions are equipped with optical sensors to monitor the environment (Belward & Skøien, 2015) providing data with diverse characteristics to meet a range of information needs. However optical data is frequently hindered by the presence of clouds and clouds´ shadows, reducing the amount of usable observations. Pixel-based image compositing has become a common practice to produce complete representations of a territory using clear observations from various dates (White *et al.*, 2014). Pixel-based compositing technique combines data from a user-restricted period (*e.g.*, a month, year, various years) and quality level into an image composite representing a specific time. Open data policies have facilitated the development of optical data analysis techniques (Wulder *et al.*, 2012) incorporating the temporal dimension into long (*e.g.*, Landsat archive with 45 years of data) or dense (*e.g.*, MODIS daily data) records. Since forests are highly dynamic systems, our understanding and assessment of resources benefit from analysis and interpretation of time series of data (Banskota *et al.*, 2014). Optical data are used by themselves or enhanced in combination with other data sources for estimation of land cover attributes, including forest distribution, condition, structure, and composition.

Hyperspectral remote sensing

Hyperspectral sensors acquire data in many—typically hundreds—very narrow bands along the electromagnetic spectrum (from the visible, near- and mid-infrared, to thermal infrared) facilitating identification of Earth surface features. Hyperspectral imagery is unique for identification of vegetation species (*e.g.*, Clark *et al.*, 2005) through spectral libraries or field references (Xie *et al.*, 2008), for monitoring forest health (Fauzi *et al.*, 2013) and environmental stressors (Schlerf *et al.*, 2010). Processing hundreds of bands and identifying the most informative ones is not straightforward (Axelsson *et al.*, 2012). To date hyperspectral data has been mainly collected from airborne platforms (*e.g.*, AVIRIS, with 224 bands) with just a few satellite missions carrying hyperspectral sensors (Transon *et al.*, 2018), among which the Earth Observing-1 (EO-1) satellite launched by NASA in 2000 carried the Hyperion sensor. Hyperion was an instrument equipped with two spectro-radiometers

acquiring VNIR to SWIR (*i.e.*, from 0.43 to 2.40 µm) data with 30 m spatial resolution and an average spectral resolution of 0.010 µm for each of its 220 functional channels (Datt *et al.*, 2003; Ungar *et al.*, 2003). EO-1 acquired data by request and was decommissioned on February 2017, with its 16 years of archived imagery remaining accessible online (https://earthexplorer.usgs.gov/). Other satellite hyperspectral missions are in study stage (*e.g.*, HyspIRI from NASA) or about to be launched (*e.g.*, EnMap from Germany).

Synthetic aperture radar (SAR)

Radar (radio detection and ranging) is an active RS technology emitting microwave pulses (1 mm-1 m) and recording the radiation backscattered from the surface. Radar has the capacity to provide data in nearly all-weather conditions, day and night (Henderson & Lewis, 1998). The radar instrument configuration—wavelength and polarizations—determines its capacity to acquire information from the ground. Different wavelengths (X-, C-, L-, and P-bands) have been used in forestry applications with success depending on objectives and analysis methods. Most synthetic aperture radar (SAR) systems have the capacity to measure the *phase*—related to the distance between the sensor and the target—and the *backscatter coefficient*—related to the target scattering properties. In forestry applications the *phase* information is often used to derive forest height, through interferometric (InSAR) or polarimetric-interferometric (PolInSAR) processing (Askne *et al.*, 2003; Garestier *et al.*, 2008) or to provide information on the dominant scattering mechanism using polarimetric decomposition techniques (Cloude & Papathanassiou 1998; Hajnsek *et al.*, 2003). Recently, multiple SAR observations acquired with a certain platform separation (baseline) are used to resolve the vertical structure of the forest using SAR tomographic processing (Tebaldini & Rocca, 2012).

The relationships between radar backscatter coefficient and forest structure were demonstrated almost three decades ago (Le Toan *et al.*, 1992). The sensitivity of radar backscatter to forest parameters increases with increasing wavelength, with P-band recognized as the most sensitive due to its greater penetration through vegetation (Dobson*et al.*, 1992; Le Toan *et al.*, 1992; Rignot *et al.*, 1994). Also, stronger relationships between the radar backscatter and forest structural properties are generally found for the cross-polarized (HV and VH) channels when compared to the co-polarized (HH and VV) channels (Le Toan *et al.*, 1992; Pulliainen *et al.*, 1994; Sandberg *et al.*, 2011; Cartus *et al.*, 2012; Shimada *et al.*, 2014). The scarcity of historical and consistently acquired radar data, especially when compared with the optical archives, precludes long retrospective analysis. However, operational satellite programmes carrying SAR instruments ensure data continuity over the next decades at least for some wavelengths. For example, the Sentinel-1 C-band mission is guaranteed until 2030 through the European Space Agency (ESA) agreements for the procurement of replacement satellites. Of particular interest for forestry, the European BIOMASS satellite mission is due for launch 2021, promising unprecedented capabilities for global assessment of forest biomass and carbon accounting from P-band data (Le Toan *et al.*, 2011), while the Japan Space Exploration Agency (JAXA) L-band PALSAR programme would continue past the current mission (*i.e.*, PALSAR-2). Among SAR missions currently in feasibility phase, the Tandem-L would provide global data for implementation of space-borne L-band PolInSAR with single-pass acquisitions, enabling forest height and height change assessment. Tandem-L could be launched in 2022 with a 10-year operational life span (Moreira *et al.*, 2015).

Light Detection and Ranging (LiDAR)

LiDAR (light detection and ranging) is an active remote sensing technology with high capacity to assist in mapping, monitoring, and assessment of forest resources (White *et al.*, 2016). RS LiDAR instruments measure the time a laser emitted beam, usually near infrared (NIR) takes to travel forth and back from the target, as one or multiple returns in the case of a *discrete return system*, or as a continuous return waveform in the case of a *full-waveform system*. The high positional accuracy granted by the Global Navigation Satellite Systems (GNSS) combined with an Inertial Measurement Unit (IMU) on LiDAR aircrafts allows the generation of three dimensional point clouds representing the spatial distribution of canopy elements, thus providing accurate measures of the vegetation's structure (Lefsky *et al.*, 1999). As any other sensor, LiDAR can be mounted on a variety of platforms: ground-based, UAV, airborne or satellite. Discrete return LiDAR systems on-board airplanes are commonly known as Airborne Laser Scanning (ALS). A key property of discrete LiDAR data is the pulse density or number of pulses reaching the surface unit. LiDAR pulse density may differ from number of points returning from the surface unit, as a function of the sensor configuration and the surface complexity. To date LiDAR is the most accurate RS technique to measure forest structure (Valbuena *et al.*, 2013b; Bottalico *et al.*, 2017) and it is typically used for predicting forest inventory attributes (González-Ferreiro *et al.*, 2012; Montealegre *et al.*, 2016; Mauro

et al., 2017a; Valbuena *et al.*, 2017b) and probability density functions (*e.g.*, Arias-Rodil *et al.*, 2018). The 3D structural information obtained from LiDAR can also be employed to characterize forest areas (Valbuena *et al.*, 2013c; 2016b) and a combination of LiDAR and optical data can efficiently complement the capabilities of each sensor (Manzanera *et al.*, 2016; Valbuena *et al.*, 2017a). The wealth of information provided by LiDAR enables forest managers to make informed and dynamic decisions at small management units (Pascual *et al.*, 2016). Despite relatively high costs of data acquisition, LiDAR is operationally used in forest inventories in some countries (Tomppo *et al.*, 2008; Hilker *et al.*, 2008).

Satellite LiDAR is expected to provide important opportunities for forest applications in the near future. From 2003 to 2009 the Ice, Cloud, and Land Elevation Satellite (ICESat) carried the Geoscience Laser Altimeter System (GLAS) sensor, providing waveform data from space with a 170 m footprint (Schutz *et al.*, 2005). Although conceived to study the evolution of land and sea glacial masses, GLAS potential and application to analyse large scale forest structure was relevant (Lefsky, 2010; García *et al.*, 2012). ICESat-2 was launched on 15th September 2018 carrying ATLAS, an improved sensor with smaller footprint (70 m). Another LiDAR sensor launched at the end of 2018 (5th December) is the Global Ecosystem Dynamics Investigation (GEDI) which will orbit the Earth on-board the International Space Station (ISS) scanning forests between 52°S and 52°N. GEDI will provide high-resolution full-waveform LiDAR data aimed to measure vegetation height, vertical structure, and bare ground elevation (Qi & Dubayah, 2016). GEDI is the first LiDAR on space mainly created to study the carbon cycle and biodiversity in forest ecosystems.

Unmanned Aerial Vehicles (UAV)

Commonly known as Unmanned Aerial Vehicles (UAV), the small Remotely Piloted Aircraft Systems (RPAS) constitute an innovative means to assist civilian applications including forest monitoring (Pajares, 2015). UAV flying space and civilian use regulations are under development worldwide. In Spain UAVs of less than 25 kg are subject to simple specific regulations by the national Agency of Aerial Safety (Agencia Estatal de Seguridad Aérea, AESA) and the latest regulatory framework was established in 2017 (RD 1036/2017). UAVs can typically fly under 120 m height and no more than 500 m from the remote pilot (Visual Line Of Sight, VLOS flying mode), although this distance can be protracted with observers (Extended Visual Line Of Sight, EVLOS). Remotely piloted vehicles may carry a number of sensors (Gómez & Green, 2017), among which conventional photographic cameras are most popular for easiness in data processing and interpretation, as well as for their low cost. Complex sensors (*e.g.*, LiDAR, hyperspectral) are generally heavier and require more power supply, restricting the number of vehicles that can carry them. Fixed-wing platforms are adequate for monitoring larger areas with a pre-defined flight plan and need space for landing, while multi-rotor platforms are better suited for manoeuvrability, having easier take-off and landing. Both types of platforms are well suited for forestry applications (Torresan *et al.*, 2017). For example, a fixed-wing vehicle equipped with multispectral (MS) sensor can repeatedly fly over the same area providing information of the forest health at different dates. A rotary wing vehicle would be more efficient and better suited to observe plots in difficult areas. Like the piloted counterparts, UAVs require very accurate location information, which is provided by an IMU and GNSS receivers. UAVs flexibility enables optimal time data acquisition, provides very high spatial resolution data, and are relatively low-cost. Photogrammetric matching algorithms mentioned before (*e.g.*, SfM, MVS) have found in UAV-based photogrammetry an extensive field for application. In comparison to ALS, UAV-based digital aerial photography is inexpensive and the point cloud can easily match ALS densities. However, the larger point density does not necessarily yield greater vertical accuracy, since it cannot penetrate vegetation (Guerra-Hernández *et al.*, 2017). Current limitations to the use of UAVs are imposed by battery duration, payload weight and local regulations (Manfreda *et al.*, 2018), as well as massive data processing capability. Although the sensor on-board a UAV defines the RS technology, we have considered UAV separately as the flying conditions impose specific characteristics to the data and processing required.

Remote sensing applications in Spanish forest ecosystems

The range of techniques outlined above, together with an increasing amount of data available and the improved storage and computing capacity offer myriad opportunities for monitoring forest ecosystems. As summarized in this section, many of these techniques have been used to monitor the Spanish forests.

Landscape characterization

Land cover (LC), land use (LU), and their changes over time are fundamental information for many

environmental applications, including assessment of carbon budgets and diversity, and characterization of forest structure and dynamics. RS offers spatially explicit and comprehensive data to get valuable insights about the land cover and use at different scales. The overall monitoring of Spanish landscapes is supported by three projects employing some form of RS: the Forest Map of Spain (Mapa Forestal Español, MFE), the Spanish Land Use Information System (Sistema de Información de Ocupación del Suelo en España, SIOSE), and CORINE (Coordination of the Information on the Environment) Land Cover.

The main objective of MFE is to support the national forest inventory. MFE has mapped the national LC three times since 1990, at scales ranging from 1:200000 to 1:25000. The most recent MFE versions are derived by photointerpretation of aerial photography and digitization of polygons with minimum mapping unit (MMU) from 0.5 ha in treed areas to 2 ha in agricultural areas. Polygons are characterized and classified according to the vegetation present in the area. MFE has a temporal frequency enough to support decadal forest inventories but too scarce for assessment of forest dynamics. SIOSE is generated to fulfil national information needs of land cover and use, with photointerpretation of satellite images and orthophotos at 1:25000 scale. The main source of data for the first SIOSE version was SPOT HGR (fusion of MS 10 m and panchromatic (PAN) 2.5 m data) complemented with aerial photography, Landsat images, and other cartographic data sources available. SIOSE is produced by manual digitization of polygons of MMU 0.5-2 ha, labelled according to a descriptive data model: polygons are not given a single label but a set of descriptors, providing flexibility for advanced interpretations. The first SIOSE was carried out in 2005, and has been updated in 2009 and 2011. CORINE LC is a continental project to map Europe from Landsat imagery. Abiding to some general guidelines, each country maps its territory with its own resources. CORINE was first developed in 1990 and has been updated in 2000, 2006, 2012, and 2018. The latest Spanish versions of CORINE are produced by generalization of SIOSE maps (García-Álvarez & Camacho-Olmedo, 2017; Martínez-Fernández *et al.*, 2019) representing a change in methodology and making the comparison with previous versions troublesome. Despite the completeness of the three mapping projects (MFE, SIOSE, CORINE) changes in very dynamic landscapes may remain undetected. However, data acquired by optical Sentinel-2 or radar Sentinel-1 could support national scale LC maps and drastically increase their frequency, enabling detailed monitoring of landscape dynamics. Although just at the scene level, the capacity of Sentinel-2 data to map land use has already been explored in Spain by Borrás *et al.* (2017) with better results obtained when compared to using SPOT images.

At the landscape level, habitat mapping is required for the European Natura 2000 conservation commitments and assessment of habitat connectivity and fragmentation is a following challenge (Hernando *et al.*, 2017). Regional efforts ongoing in Castilla y León (Bengoa *et al.*, 2017) or Cantabria (Álvarez-Martínez *et al.*, 2017) combine optical, LiDAR, and ancillary data to classify and map vegetation types with machine learning techniques. Gastón *et al.* (2017) recently compared the performance of PNOA LiDAR, MFE data, and CORINE data to assess forest habitat suitability for brown bears across the Cantabrian Range employing canopy cover variables. Object-based image classification techniques—in which the basic unit is a group of spectrally similar pixels rather than the pixel itself—combining aerial multispectral imagery and LiDAR data from PNOA were used by Hermosilla *et al.* (2012) to characterize forest abandoned lands. In addition, texture information from spectral bands may improve accuracy in land cover classification (*e.g.*, Ruiz *et al.*, 2005). Data fusion combining SPOT 6, Landsat 8, and Terra MODIS data was also crucial in describing spatial landscape heterogeneity to identify forested and human modified areas by Silveira *et al.* (2018).

Evidence on species composition is needed to inform silvicultural prescriptions, biodiversity or other management needs. Although traditional RS approaches to characterize tree species dominance have had variable success (Fassnacht *et al.*, 2016; White *et al.*, 2016), improved results were obtained with multi-date or time series analysis. Gómez *et al.* (2018) have recently mapped the distribution of *Fagus sylvatica* L. (European beech) in the Central Range, based on a multi-date classification of Landsat OLI data. Beech species, considered relict in the area, is expanding as indicated by the comparison of current and previous cartographic records as well as field verification measurements. To estimate changes in species dominance in Ordesa National Park a 33 year annual series of Landsat data classified with support vector machine was used by Gómez *et al.* (2016a), corroborating trends in *F. sylvatica* L., *Abies alba* Mill., and *Pinus sylvestris* L. recent dynamics (Camarero *et al.*, 2011; Sangüesa-Barreda *et al.*, 2015). Combining field data and time series of Tasseled Cap Wetness values (a linear combination of spectral bands which is indicative of water content) in a geostatistical model Aulló-Maestro *et al.* (2017) confirmed a change in species dominance in Pinar de

Hoyocasero (Ávila) that will affect local biodiversity (Rubio *et al.*, 2011). Coarser spatial resolution data from MODIS has been employed to discriminate pine species by differences in phenology (Aragonés *et al.*, 2017). The authors modelled 368 16-day composites of data acquired in 2000-2016—spatially stratified by field data from the National Forest Inventory—and characterized curve patterns corresponding to five pine species classified with >70% accuracy.

Quantification of resources

In Spain as in many other countries the National Forest Inventory (NFI) is an effort to keep forest resources (*e.g.*, volume, biomass) assessed periodically, providing base information for decision making, forest management, and research. The Spanish NFI (SNFI) is based on a 1×1 km network of permanent field plots measured every ten years. The high cost of measurements precludes more frequent updates, making the sole use of SNFI data imperfect for current reporting needs. SNFI represents a robust database reliable as reference for calibration and validation of forestry studies and applications based on RS datasets. For instance, González-Alonso *et al.* (2006) estimated biomass at national level calibrating their models with data from the SNFI 2nd rotation, and Gómez *et al.* (2014) modelled and assessed biomass and change of biomass in pines of the Central Range with Landsat time series calibrated with data from the 2nd (ca. 1990) and 3rd (ca. 2000) SNFI rotations. Other authors have found useful the integration of SNFI and SAR data for estimation of biomass (Joshi *et al.*, 2017) and SNFI and LiDAR data for estimation of canopy fuel (González-Ferreiro *et al.*, 2017) and structural parameters (Fernández-Landa *et al.*, 2018).

The nationally available LiDAR data from PNOA has been operationally used for forest inventory from management unit to forest scale (100-10000 ha), and some online tools have been developed to facilitate access to volume estimates or fire models. Some examples are GINFOR for Castilla la Mancha (Blanco-Martínez *et al.*, 2017) or Forestmap, which is currently available for 11 provinces (Fernández-Landa *et al.*, 2017; Tomé *et al.*, 2017). This kind of tool requires basic input from the user, like selecting an area of interest, and facilitates rapid estimations for decision making. LiDAR allows extraction of individual tree attributes through individual tree crown (ITC) approaches (Hyyppä & Inkinen, 1999) and estimation of stand-level variables using the area based approach (ABA) (Næss et, 2002; White *et al.*, 2013) or Empirical Best Linear Unbiased Predictors (EBLUPs) (Mauro *et al.*, 2016). The PNOA LiDAR dataset was tailored for topographic applications, and its low point density may limit forestry applications such as structural characterization of dense forests (Adnan *et al.*, 2017). Nonetheless, many important inventory variables (*e.g.*, height, density) can be estimated with sufficient accuracy for certain purposes when there are enough ground returns to retrieve an accurate DTM, by choosing the appropriate relation between LiDAR pulse density and plot size (Ruiz *et al.*, 2014). Although high density (> 3 pulse × m^{-2}) LiDAR is expensive, some regional administrations in cooperation with the National Geographic Institute have acquired this quality of LiDAR data (*e.g.*, Navarra: 14 pulse × m^{-2}; Basque Country and La Rioja: 2 pulse × m^{-2})—superior to densities typically found in national programmes in countries with highly productive forest resources, such as Finland (Valbuena *et al.*, 2016a)—that may provide more accurate estimates in dense forests.

When forest inventories require estimates of structural attributes at stand or sub-stand level (0.5-50 ha) with relative errors below 5-10% (*e.g.*, for management purposes; Pascual *et al.*, 2018b), ABA LiDAR assisted methods become economically unaffordable due to the need of sufficient field data. To address this problem Mauro *et al.* (2016) implemented *small area estimation* approaches to a LiDAR-assisted inventory in a *Pinus pinaster* Ait. forest in Burgos. Mauro *et al.* (2016, 2017a, 2017b) based their estimations on EBLUPs using LiDAR data as auxiliary information, and demonstrated this approach is more accurate than traditional inventories over small areas. Additionally, with this approach area level models just require identification of the plot/stand correspondence and an accurate location of plots is not needed. Thus, the SNFI plot positioning difficulty no longer applies (Mauro *et al.*, 2011; Valbuena *et al.*, 2012; Pascual *et al.*, 2018a), enhancing the EBLUP methods the value of SNFI and PNOA LiDAR for operational forest inventories.

Focussing on biomass and carbon budgets—necessary for monitoring management practices and for reporting to international commitments (Montero *et al.*, 2005; Ruiz-Peinado *et al.*, 2011)—a host of RS techniques and data types have been employed in Spanish forests during the recent decades (Table 2). González-Alonso *et al.* (2006) estimated forest biomass over the entire country at the province level with Normalized Difference Vegetation Index (NDVI) composites from SPOT VEGETATION and NOAA-AVHRR, and SNFI plots. This approach is useful for overall reports but lacks enough detail for management or local assessment. In a more detailed scale, optical images from the Advanced Spaceborne Thermal Emission and

Table 2. Examples of works for estimation of biomass and carbon fluxes with remote sensing in Spanish forest ecosystems.

Reference	Variable	Data source	Area (km^2)	Forest type	Approach	Error/accuracy
García *et al*., 2010	Biomass: foliage branches total	LiDAR (1.5-4.5 pulse × m^{-2})	382	*Pinus nigra, Juniperus thurifera* and *Quercus ilex*	Regression (stepwise)	RMSE: 1.12 T × ha^{-1} 15.27 T × ha^{-1} 17.82 T × ha^{-1}
Estornell *et al*., 2011a	Biomass	LiDAR (4 pulse × m^{-2})	10	*Quercus coccifera*	Regression	RMSE = 34.7% (1.45 kg)
Gómez *et al*., 2012a	Carbon change	Landsat TM, ETM+	10000	Coniferous	Time series 1984-2009	N/A
Sevillano-Marco *et al*., 2013	Biomass	CBERS ASTER	150	Coniferous	Regression	RMSE = 39.9%
Estornell *et al*., 2012	Biomass	LiDAR (4 pulse × m^{-2}) MS image	10	*Quercus coccifera*	Regression	RMSE = 22% (96.55 kg)
González-Ferreiro *et al*., 2013a	Biomass: crown stem total	LiDAR (4 pulse × m^{-2})	4	*Eucalyptus globulus*	Regression	RMSE: 3.5 T × ha^{-1} 19.9-25.9 T × ha^{-1} 23.2-30.1 T× ha^{-1}
Fernández-Manso *et al*., 2014	Biomass	ASTER	68.5	Coniferous	Fraction images	RMSE = 37.7%
Gómez *et al*., 2014	Biomass dynamics	Landsat TM, ETM+	814	Coniferous	Time series 1984-2009	70% accuracy
Tanase *et al*., 2014a	Biomass	ALOS PALSAR	134	Coniferous	Parametric / non-parametric	RMSE = 60-80% (21±2.2 T × ha^{-1})
Méndez *et al*., 2016	Biomass	ALOS PALSAR	210	Coniferous and broadleaved	Regression	RMSE = 39-51%
Guerra-Hernández *et al*., 2016	Biomass: stem crown total	LiDAR (0.5 pulse × m^{-2})	7.48	*Pinus pinea, Quercus pyrenaica,* and mixed	Regression (stepwise)	RMSE (*P. pinea*): 26.16% 25.89% 25.90%
Domingo *et al*., 2017	Biomass loss and CO_2 emissions	LiDAR (1.5 pulse × m^{-2})	142/ 33.9	*Pinus halepensis*	Regression (multiple linear) Random Forest Support Vector Machine Decision Tree	RMSE = 11.1%
Montealegre *et al*., 2017b	Biomass loss and CO_2 emissions	LiDAR (1 pulse × m^{-2})	82.7	*Pinus halepensis*	Regression (forward stepwise)	RMSE = 27.35%
Navarro-Cerrillo *et al*., 2017	Total aboveground biomass	LiDAR (4 pulse × m^{-2})	N/A	*Pinus sylvestris Pinus nigra*	Regression (multiple linear)	RMSE: *P. sylvestris* = 2.89% *P. nigra* = 0.38%
Trassierra *et al*., 2017	Biomass	LiDAR (0.5 pulse × m^{-2}) Landsat OLI	N/A	*Cistus laurifolius*	Regression Random Forest	RMSE: (LiDAR) = 26.75% (Landsat) = 41%
Valbuena *et al*., 2017b	Biomass	LiDAR (1.15 pulse × m^{-2}) and MS-DAP	8	*Pinus sylvestris*	Most similar neighbour	RMSE = 14.4 %
Hernando *et al*., 2019	Biomass: foliage branches total	LiDAR (1.15 pulse × m^{-2}) and MS-DAP	8	*Pinus sylvestris*	Most similar neighbour	RMSE: 19.99 % 18.21 % 16.72 %

Reflection Radiometer (ASTER) images were used by Fernández-Manso *et al.* (2014) to estimate biomass of pines in Segovia. A combination of the red and SWIR bands with the green fraction obtained applying Linear Spectral Mixture Analysis (LSMA) yielded the strongest relationship with biomass (R = 0.63). LSMA was applied to lessen the effect of mixed pixels and showed a positive contribution in the modelling. Gómez *et al.* (2012a) described changes in carbon content at the landscape level in pines of the Central Range employing a time series of Landsat images (8 images for a 25-year period). Through interpretation of the temporal derivative of the time series—named Process Indicator (PI)—the rates and directionality of change (*i.e.*, increase or decrease) were characterized. The same Landsat series served a 2D wavelet transformation model calibrated with SNFI plots for estimation of biomass dynamics (Gómez *et al.*, 2014), whereby changes in biomass were mapped with 70% accuracy. In general, the biomass of Spanish forests has proven difficult to characterize with spectral traits (Vázquez de la Cueva, 2008) in part due to their heterogeneity and location in rugged areas. Such factors, added to the saturation of optical and radar sensors, preclude accurate estimation of high values of biomass. LiDAR technology has become key for assessment of aboveground forest biomass, enabling estimation of its distribution among crowns, trunks, branches and leaves, and quantification of biomass loss and CO_2 emissions (Table 2).

National Parks Administration (Organismo Autónomo de Parques Nacionales, OAPN) currently monitors the net primary production (NPP) of ecosystems in National Parks with REMOTE, an application for analysis of MODIS NDVI and EVI (Enhanced Vegetation Index) time series (Cabello *et al.*, 2016). Information of the NPP contributes to inform about the National Parks state of conservation. The high frequency of continuous data and accumulated reference data facilitates an alarm system for identification of anomalies as well as characterization of tendencies. Cicuéndez *et al.* (2015) demonstrated that the NASA derived MODIS Gross Primary Production (GPP) product (MOD17A2, 1 km spatial resolution) underestimates dehesa GPP due to ecological parameters such as soil moisture and precipitation. For such finding the authors compared 5 years (2004-2008) of MOD17A2 with a MODIS-based locally calibrated GPP in a 600 ha holm-oak dehesa in Cáceres.

Shrub ecosystems—18.4 million ha in Spain, MAPAMA 2011—have attracted efforts for estimation of biomass and volume. Estornell *et al.* (2011a) employed high density LiDAR (average 8 point × m^{-2}) to evaluate biomass of a *Q. coccifera* dominated area in Chiva (Valencia) and obtained accurate results (R^2 = 0.73) in plots of 1.5 m radius when a highly accurate Digital Terrain Model (DTM) (RMSE < 0.2 m) was employed. Biomass estimates over the same area were improved by combining LiDAR with spectral data from an airborne flight and when assessing results in squared plots of 100 m^2 (Estornell *et al.*, 2012). Trassierra *et al.* (2017) estimated *Cistus laurifolius* L. aerial biomass in experimental plots (11.3 m radius with subplots of 2 m radius) in Soria and compared models based on PNOA LiDAR or Landsat variables. The authors found better results when building parametric models with LiDAR data, but Landsat spectral information was considered as an acceptable alternative.

Although information from SAR images is particularly complex to retrieve in fragmented landscapes with steep topography, as frequently found in Spanish forests, SAR images have demonstrated potential for estimation of aboveground biomass (Tanase *et al.*, 2014a; Joshi *et al.*, 2017). Tanase *et al.* (2014a) used SNFI plots to evaluate parametric and non-parametric modelling retrieval of biomass as a function of dual-polarized (HH, HV) ALOS PALSAR backscatter of coniferous forests in Aragon. The study concludes that observed errors obtained with non-parametric models are similar and that within the sensitivity interval of the L-band wavelength (10-100 T × ha^{-1}) biomass estimates are relatively accurate (RMSE = 20-35%). Considerably larger errors were observed outside this interval since at low biomass levels (<10 T × ha^{-1}) backscattering largely depends on surface properties while at high biomass levels (>100 T × ha^{-1}) signal saturation sets in. Méndez *et al.* (2016) used ALOS PALSAR for estimating eucalyptus and pine forest biomass in Huelva by modelling the relationship between the backscatter coefficients and wood volume. Correlations were high (R = 0.7-0.8) but so was the relative error (RMSE = 39.8-51.6%). The signal saturation point was identified at 100 T × ha^{-1} suggesting that improved modelling approaches are needed to meeting forest management needs, a conclusion also reached in other studies over similar environments (Tanase *et al.*, 2014b). Joshi *et al.* (2017) found that the inclusion of forest structural information is crucial to establishing suitable relationships between stand volume or biomass and SAR backscatter, and using that approach mapping forests with SAR images may not need to be restricted to areas with low biomass.

Structural characterization

Characterizing structural parameters like dominant height or basal area at different scales—individual tree,

plot, stand, landscape—employing diverse techniques and datasets is a typical RS effort (Table 3). Very high spatial resolution (0.7-2.4 m pixel size) data from single date QuickBird-2 images were employed by Gómez *et al.* (2012b) to estimate quadratic mean diameter, basal area, and number of trees per hectare in pine areas of the Central Range. In the same areas Gómez *et al.* (2011) modelled the stand structural diversity and found that image texture variables make a valuable contribution in structural modelling. The advent of LiDAR technology since the beginning of the century has reduced estimation error, marking a milestone change in this field (Table 3). At local scale UAVs can be used for estimation of tree heights (Zarco-Tejada *et al.*, 2014), with an on-board LiDAR or from DAP point clouds. However, the DAP technology is not yet operationally used in the Spanish forest sector, although it has shown valuable for estimation of structural parameters with accuracies similar to those from LiDAR when an accurate DTM is available (Navarro *et al.*, 2018).

LiDAR data by itself or in combination with other data sources have demonstrated capacity for assessment of the main forest structural variables (*i.e.*, height, basal area, volume) and also a number of derived forest properties (*e.g.*, complexity, diversity, regeneration) (Table 3). For example, Fernández-Landa *et al.* (2018) estimated basal area, volume, and number of stems per hectare in pine and beech forests of La Rioja with PNOA LiDAR data and SNFI plots, and Gonçalves-Seco *et al.* (2011) estimated canopy cover, density, and tree height in dense stands of eucalyptus plantations in Galicia. Estornell *et al.* (2011b) predicted dominant height of *Quercus coccifera* L. in Chiva (Valencia) from discrete LiDAR metrics with accuracy ($R^2 = 0.73$), while Crespo-Peremarch *et al.* (2018) characterized understory vegetation attributes (*i.e.*, mean and maximum height, cover, and volume) at the plot level employing full-waveform LiDAR metrics in Sierra de Espadán (Castellón). ITC approaches have sometimes been used for measurement of individual tree height (*e.g.*, González-Ferreiro *et al.*, 2013b in *P. radiata* plantations in Galicia), but ITC approaches are more sensitive to pulse density than ABA and there fore less employed in forest inventories. Although discrete LiDAR returns below 1.5-2 m are frequently considered signal noise and dismissed—leaving shrub structure below this height unaccounted for—some studies have focused on the structure of forest lower layers, including regeneration stages. Valbuena *et al.* (2013c) showed the relationship of under-canopy parameters to other forest structural properties and employed these relationships to unravel the success of natural regeneration in *P. sylvestris* forests of Valsaín (Segovia). Blázquez-Casado *et al.* (2015) studied forest dynamics and regeneration after storm damage with 2011 acquired LiDAR (≥ 6 pulse × m^{-2}) and historical (1956/1977/1996) aerial photography, showing how natural disturbances influence forest development. Simonson *et al.* (2018) explored the effects of phenology on LiDAR metrics in mixed stands of *Quercus suber* L. and *Quercus canariensis* Willd. in Los Alcornocales Natural Park (Cádiz). Employing two spring datasets acquired in a six week interval, there was consistency in the maximum and mean height estimations but some differences in standard deviations and skewness. Combining data from multiple sensors usually provides important synergies for the characterization of forest structure (Pascual *et al.*, 2010; Manzanera *et al.*, 2016; Ruiz *et al.*, 2018). However, Valbuena *et al.* (2017a) obtained mixed results when combining LiDAR with MS information from DAP, suggesting that synergies among sensors may be beneficial in some cases but counterproductive for structural variables that just depend on vegetation heights.

Mapping the structural complexity, that is, structural types and development stages of forests helps decision making. Pascual *et al.* (2008; 2013) developed a two-stage method for depicting forest structural types of *P. sylvestris* stands in the Central Range. Attending to an increasing participation of forest management expert opinion, the best classification of structural types was obtained from a fully automatic delineation of stands with LiDAR data—by means of an object-oriented segmentation algorithm—with subsequent k-means clustering of stands into five structural types. Automated methods developed from LiDAR data to describe forest structural types in Spain (Valbuena *et al.*, 2013c) have recently been extended for a more generalized use across ecotypes in Europe (Adnan *et al.*, 2018).

There has been an intense research effort for optimization of methods employing LiDAR data in the assessment of structural properties in Spanish forests. The influence of pulse density—a key variable when acquiring LiDAR data—has received particular attention. In 2012 González-Ferreiro *et al.* evaluated a range of pulse densities (0.5-8 pulse × m^{-2}) for estimation of height, basal area, and volume of *Pinus radiata* D. Don. plantations in Galicia, and found similar performances. Varo-Martínez *et al.* (2017) evaluated the capacity of (0.5/4.0/10.5 pulse × m^{-2}) LiDAR data in the delineation of *P. sylvestris* stands in Sierra de Los Filabres (Almería) and found no significant difference, but for estimation of height the densest dataset performed best. On the contrary, Marino *et al.* (2017a) found similar performance in the estimation of

Table 3. Examples of forest structural characterization in Spain employing remote sensing

Reference	Structural variable	Data	Forest type	Approach	Error
Pascual *et al.*, 2008 Pascual *et al.,* 2013	Structural types	LiDAR Landsat	Pines 120 ha	Object classification Regression	N/A
Estornell *et al.,* 2011b	Ho	LiDAR (4 pulse × m^{-2})	*Quercus coccifera*	Regression	RMSE= 0.13 m
Gómez *et al*., 2012b	QMD, G, N	QuickBird-2	Pines 13000 ha	CART Stand level characterization	RMSE: QMD = 0.13 m G = 5.79 $m^2 \times ha^{-1}$ N = 98.86
González-Ferreiro *et al*., 2012	G, V, Ho, Hm	LiDAR (8 pulse × m^{-2})	*Pinus radiata* 3600 ha	Regression	RMSE: G = 7.8 $m^2 \times ha^{-1}$ V = 76.9 $m^3 \times ha^{-1}$ Ho = 1.88 m Hm = 1.92 m
Sevillano-Marco *et al*., 2013	G, V	CBERS and ASTER	*Pinus radiata* 693.9 ha	Non-linear Regression	RMSE: G = 19.9 $m^2 \times ha^{-1}$ V = 214.2 $m^3 \times ha^{-1}$
Condés *et al*., 2013	V	LiDAR (2 pto× m^{-2})	*Pinus sylvestris* 1121 ha	Two-phase regression	Relative error = 5.1 %
Valbuena *et al.*, 2013b	G, N	LiDAR (1.15 pulse × m^{-2})	*Pinus sylvestris* 384 ha	PLS regression and multimodel inference	RMSE: G = 9.06% N = 18.04%
García-Gutiérrez *et al*., 2014	G, Ho, Hm	LiDAR (0.5-8 pulse × m^{-2})	*Eucalyptus globulus* *Pinus radiata*	Genetic approach MLR	RMSE: G = 8.51/7.60 $m^2 \times ha^{-1}$ Ho = 2.01/1.89 m Hm = 1.71/1.86 m
Ruiz *et al*., 2014	G, V, CC	LiDAR (0.25-6 pulse × m^{-2})	*Pinus nigra* *Pinus sylvestris*	Regressions; adaptive threshold	Variable RMSE depending on pulse density and plot sizes used.
Blázquez-Casado *et al*., 2015	G, Hm, N, cover, Nm, Dm, Do, RD_H to define structural types	LiDAR (6 pulse × m^{-2})	*Pinus uncinata* 208 ha	Aggregation of individual tree metrics into stand level structural variables to define forest types	N/A
Manzanera *et al*., 2016	V, Hl, SDI, GC, La, BALM	LiDAR (1.15 pulse × m^{-2}) MS imagery	*Pinus sylvestris* 4.6 ha	Back-p rojecting and canonical correlation analysis	Canonical R^2 = 98.9
Montealegre *et al*., 2016	G, Hm, QMD, N	LiDAR (PNOA) (1 pulse × m^{-2})	*Pinus halepensis*	Multiple regression	RMSE: Hm = 0.72 m QMD = 1.99 cm G = 2.39 $m^2 \times ha^{-1}$ N = 187 stem × ha^{-1}

Table 3. Continued.

Reference	Structural variable	Data	Forest type	Approach	Error
Fernández-Landa *et al.*, 2018	G, N	LiDAR (0.5 point × m^{-2}) SNFI, Landsat	*Pinus sylvestris* *Fagus sylvatica* 16000 ha	Area based approach GLM modelling	RMSE: G_{beech} = 6.9 $m^2 \times ha^{-1}$ G_{pine} = 3.3 $m^2 \times ha^{-1}$ N_{beech} = 361 stem × ha^{-1} N_{pine} = 392 stem × ha^{-1}
Arias-Rodil *et al*., 2018	QMD, Dm	LiDAR (PNOA) (0.5 pulse × m^{-2})	*Pinus radiata*	Regression	RMSE: QMD = 3.42 cm Dm = 3.62 cm
Crespo-Peremarch *et al.*, 2018	Understory: V, Hm, Hmax, cover	LiDAR full-waveform (14 pulse × m^{-2})	Shrub under *Pinus halepensis, Pinus pinaster*	Regression	RMSE: V = 56.49 $m^3 \times ha^{-1}$ H_m = 0.08 m H_{max} = 0.51 m cover= 9 %
Navarro *et al*., 2018	G, V, Ho, N	DAP from PNOA imagery (4.32 point × m^{-2}) LiDAR (2.96 point × m^{-2})	*Pinus pinaster* 1926 ha	Random Forest	RMSE: G = 27.02% V = 26.80% Ho = 10.71% N = 43.02%

Note. G: basal area; V: volume; CC: canopy cover; QMD: quadratic mean diameter; Dm: mean diameter; Hm: mean height; Ho: dominant height; Hl: Lorey´s height; N: stem density; SDI: stand density index; GC: Gini coefficient; La: Lorenz asymmetry; BALM: proportions of basal area larger than the QMD; Nm: Recruitment with D between 2.5 and 7.5 cm; RD_H: relative difference between dominant and mean height.

P. sylvestris height in Valsaín (Segovia) when comparing 0.5 with /1.5-5.0 pulse × m^{-2} LiDAR data, but the lower strata was better characterized with denser point clouds. Ruiz *et al.* (2014) analysed the combined effect of plot size and LiDAR pulse density on estimates of volume, biomass, basal area, and canopy cover in pines of the Central Range (Cuenca). The authors found that the rate of improvement in model estimates decreases when using plot areas ≥ 500-600 m^2, while densities >1 pulse × m^{-2} do not significantly improve predictions. The variety of sometimes apparently opposite results suggests there is no general optimal LiDAR data density, but it rather depends on the work objectives and structure of the target forest. A good choice of LiDAR predictive variables is relevant when modelling forest structure (García-Gutiérrez *et al.*, 2014; Valbuena *et al.*, 2017b), and the estimation and classification methods may also play a significant role (Guerra-Hernández *et al.*, 2016; Valbuena *et al.*, 2016b; Domingo *et al.*, 2017, 2018). Regarding the scale of data aggregation, Mauro *et al.* (2016) showed that it has important consequences and demonstrated the subsequent trade-offs with the desired accuracy in the estimation of forest structural variables.

Fire assessment

Remote sensing technology has extensively been used for fire related applications in Spain, including identification of area burned and fire severity, characterization of fire drivers, and monitoring regeneration (Table 4). A burned forest area can be determined by classification of a single post-fire image (Quintano *et al.*, 2006) since the spectral signature of burned vegetation has higher visible and SWIR values and lower NIR values compared with non-burned areas. However, differential approaches (*i.e.*, temporal comparison) and active fire information based on thermal anomalies are more reliable for large and heterogeneous areas. Merino de Miguel *et al.* (2010) successfully applied a scar detection algorithm based on MODIS active fire data and a single MODIS post-fire infrared reflectance image (500 m) in Galicia, making use of freely available and highly processed products and without needing field data. Deepening on this cost-effective method and working on the same area, Huesca *et al.* (2013a) demonstrated similar mapping results employing MERIS post fire infrared reflectance data (300 m), and certainly higher accuracies than achieved by global fire products. Overall, these low spatial resolution datasets have great value for regional assessments, although they lack sufficient spatial detail for management. With fine spatial detail Verdú & Salas (2010) compared four pairs of Landsat and SPOT composites for the period 1991-2005 at irregular intervals of 1-5 years and visually identified and mapped fire scars over Spain. As expected the total area burned by fires larger than 100 ha was better correlated with the official fire database in the shortest interval product (1999-2000) than in other 5-year interval products. But mapping fire scars at large scale with fine temporal frequency and spatial resolution

Table 4. Examples of forest fire related remote sensing applications in Spain.

AREA BURNED		
Study	**Data**	**Techniques**
Quintano *et al*., 2006	NOAA AVHRR and Landsat	Classification of fraction images
Verdú & Salas, 2010	Landsat and SPOT	Visual analysis
Merino de Miguel *et al*., 2010	Active fire data and MODIS (500 m) reflectance	Threshold correlation
Huesca *et al*., 2013a	Active fire data and MODIS (250 m)/ MERIS (300 m) reflectance	Threshold correlation
Gómez *et al.*, 2017	Landsat time series (TM, ETM+)	Trend analysis of NBR with C2C algorithm
Belenguer-Plomer *et al.*, 2018	Sentinel-1 time series	Change detection, Reed-Xiaoli anomaly detection, Random Forests
FIRE SEVERITY		
Study	**Data**	**Techniques**
Álvarez-Taboada *et al.*, 2007b	Landsat-TM	OBIA Thresholding
De Santis & Chuvieco 2007	Landsat-TM	Radiative transfer model inversion simulations
Chuvieco *et al*., 2007	Landsat-TM, Terra-MODIS, SPOT-HRV, Envisat-MERIS, IRS-AWIFS	Radiative transfer model inversion simulations
De Santis & Chuvieco 2009	Landsat-TM and SPOT5-HRG	Spectral Angle Mapper supervised classification
Tanase *et al*., 2010a	ERS 1/2, ENVISAT ASAR, TerraSAR-X,	Radar backscatter
Tanase *et al*., 2010b	ALOS PALSAR	Radar coherence
Tanase *et al*., 2011a	Landsat TM	Change detection
Tanase *et al*., 2014c	Radarsat-2, ALOS PALSAR	Polarimetric decomposition
Tanase *et al.*, 2015a, b	ALOS PALSAR, Landsat TM	Change detection
Quintano *et al*., 2015	Landsat ETM+	Correlation and regression of Land Surface Temperature and CBI
Viedma *et al*., 2015	Landsat TM	Relative Differenced Normalized Burn Ratio and Boosted regression tree analysis
Fernández-Manso *et al*., 2016a	Sentinel-2A	Multinomial logistic regression
Montealegre *et al*., 2017a	LiDAR PNOA (0.5 pulse × m^{-2})	Logistic Regression
Botella-Martínez & Fernández-Manso, 2017	Landsat 8 OLI	Threshold classification of NBR derived indices
Fernández-García *et al.*, 2018	Landsat 8 OLI/TIRS, ETM+	Linear Regression
Quintano *et al*., 2018	Sentinel-2A MSI, Landsat 8 OLI	Threshold classification of NBR derived indices
FUEL TYPE AND STRUCTURE		
Study	**Data**	**Techniques**
Riaño *et al*., 2002	Landsat TM and DEM-derived data	Supervised classification (maximum likelihood)
Arroyo *et al*., 2006	QuickBird-2	OBIA classification
González-Olabarría *et al*., 2012	LiDAR (2 pulse × m^{-2})	FlanMap simulation
González-Ferreiro *et al.*, 2014	LiDAR (0.5 point × m^{-2})	Regression
Marino *et al*., 2016	LiDAR(1 pulse × m^{-2}) and Landsat 8 OLI	Vegetation classification and fuel model assignment
Alonso-Benito *et al.,* 2016	LiDAR(2.43 point × m^{-2}) and WordView2	OBIA classification
Robles *et al.*, 2016	LiDAR(2 point × m^{-2}) and aerial images	OBIA classification
Hevia *et al*., 2016	LiDAR (8-16 point× m^{-2})	Regression
Marino *et al*., 2018	LiDAR (1 pulse × m^{-2}) and ForeStereo	OBIA classification
Arellano-Pérez et al., 2018	Sentinel-2A	Random Forest and Multivariate Adaptive Regression Splines

Table 4. Continued.

FUEL MOISTURE		
Study	**Data**	**Techniques**
Chuvieco et al., 2002	Landsat-TM	Multi-temporal analysis
Chuvieco et al., 2004a	NOAA14 AVHRR	Regression and trend interpretation
Chuvieco et al., 2004b	Landsat TM, SPOT Vegetation, NOAA14 AVHRR	Regression and trend interpretation
Yebra & Chuvieco 2009	MODIS	Look Up Table
RECOVERY		
Study	**Data**	**Techniques**
Vicente-Serrano 2011	Landsat time series (TM, ETM+)	Trend analysis of NDVI
Tanase *et al.*, 2011b	ENVISAT ASAR, TerraSAR-X, ALOS PALSAR	Trend analysis
Huesca *et al*., 2013b	MODIS and AHS	Time series of NDVI (MODIS) Spectral unmixing (AHS)
Fernández-Manso *et al*., 2016a	Landsat time series (TM, ETM+)	Trend analysis of a Vegetation Recovery Index defined from MESMA fraction images
Martínez *et al*., 2017	Landsat TM, ETM+	Trend analysis of TCW with LandTrendr algorithm
Viana-Soto *et al*., 2017	Landsat TM, ETM+	Ordinary Least Squares and Geographic Weighted Regression between NDVI and CBI
Marino *et al*., 2017b	LiDAR (1 pulse × m^{-2})	Comparison of structural metrics pre- and post-fire
Debouk *et al*., 2013	LiDAR (0.7 pulse × m^{-2})	Artificial Neural Network

using RS techniques requires automatic approaches. In this sense, Bastarrika *et al.* (2014) developed semi-automatic software named Burned Area Algorithm Software (BAMS) for identification of burned areas based on threshold values of various spectral indices. BAMS supports the use of Landsat TM, ETM+, and OLI images and works on ArcGIS environment. Recently time series approaches are preferred to bi-temporal approaches for their effectiveness and temporal accuracy in identifying fire occurrence. Gómez *et al.* (2017) tested Composite2Change (C2C), a change identification algorithm based on trend analysis, to reconstruct 31 years (1985-2015) of annual fires in Northern Spain. C2C (Hermosilla *et al.*, 2015, 2016) was developed for analysis of forest change in Canada, and it analyses the Normalized Burn Ratio (NBR) trajectory of individual pixels of Landsat composites, identifying an abrupt decrease of values in the trend as a change, and aggregating neighbouring pixels with similar trend into polygons. Furthermore, the object-oriented approach usually performs better than pixel-based approaches when mapping burned area and severity, as shown by Álvarez-Taboada *et al.* (2007b) using Landsat TM data.

Burn severity is frequently estimated fitting ground reference data—*e.g.*, the Composite Burn Index (CBI, Key & Benson, 1999) a semi-quantitative index of severity—and RS variables from a range of data sources (De Santis & Chuvieco, 2007). In order to understand the causes of variability in spectral response with variations in burn severity, Chuvieco *et al.* (2007) simulated factors like soil background, leaf colour, and leaf area index, and compared models of burn severity produced with various sensors (Table 4). Landsat-TM provided the best compromise between spectral and spatial resolution and it best fitted the measured and observed CBI values. Burn severity models are typically more reliable in estimation of high than intermediate or low severity levels, both working at regional (Tanase *et al.*, 2011a) or local scale (De Santis & Chuvieco, 2009). Viedma *et al.* (2015) used Landsat data to estimate severity in burned pines in Guadalajara (>12600 ha) and identified burning conditions like weather, propagation direction or rate of spread, as more relevant factors driving severity than pre-fire stand structure and directional topography. Temperature measured from a series of post-fire Landsat ETM+ datasets was tested as indicator of burn severity by Quintano *et al.* (2015) evidencing that surface temperature is strongly related with ground CBI values, thus proving its value to understand fire severity patterns. Fernández-Manso *et al.* (2016a) employed Sentinel-2A data to discriminate four levels of burn severity in Sierra del Teleno, demonstrating the superiority of the red-edge

indices for this purpose, in agreement with Huang *et al.* (2016) who found the 20 m MSI NIR, red-edge, and SWIR bands best for mapping burned areas in different vegetation formations around the Globe. Aiming to evaluate the capacity of LiDAR data, Montealegre *et al.* (2017a) modelled and mapped burn severity in four large fires (> 500 ha) in Aragon with PNOA LiDAR data. Correlations between LiDAR and field measured CBI were comparable to those between Landsat-based NBR maps and CBI. Hyperspectral imagery has also demonstrated capacity to estimate burn severity, from the satellite platform Hyperion (Parra & Chuvieco, 2005), and from an aerial platform (Huesca *et al.*, 2013b), but the scarcity of data makes this type of sensor less attractive for the purpose. On the contrary, over the past decade SAR-based retrieval of fire impacts has received significant attention over Spanish forests and the potential of radar sensors has been demonstrated for all wavelengths (X-, C-, and L-bands) available on satellite platforms. The variables and approaches implemented are diverse, including a range of SAR metrics from backscatter coefficient (Tanase *et al.*, 2010a), interferometric coherence (Tanase *et al.*, 2010b) and polarimetric decomposition (Tanase *et al.*, 2014c). A combination of active and passive datasets in a multi-temporal change detection approach was also proposed in an operational framework for rapid fire impact assessment at regional to continental scales (Tanase *et al.*, 2015a, 2015b). The framework was tested in various locations in Spain as well as in Australia and the US and it is based on the Radar Burn Ratio (RBR), an index pre-calibrated with in situ data.

Evaluating fire risk and danger requires knowledge of the fuel type and its moisture content, as well as factors like climate and topography. Certainly at large scale these factors are best estimated or modelled with some RS support. Riaño *et al.* (2002) generated a fuel type map of Cabañeros National Park with a supervised classification of Landsat data, getting the global accuracy considerably increased—from 67.3% to 79.4%—when illumination and slope were considered. Arroyo *et al.* (2006) demonstrated the usefulness of very high spatial resolution data to map fuel types by classifying optical data from QuickBird-2 (0.7-2.4 m) and mapping six vegetation structural types in Madrid with an overall accuracy of 80%. To predict the potential type of wildfire (surface, passive-crown, active-crown fire) at large scale, Arellano-Pérez *et al.* (2018) employed Sentinel-2 data over homogeneous plantations of *P. radiata* and *P. pinaster* in Galicia. A main limitation of spectral data for fuel type mapping is the inability to penetrate forest canopies (Keane *et al.*, 2001) and to provide direct estimation of vegetation height. On the contrary, LiDAR airborne data can successfully be used to estimate critical canopy fuel parameters (*e.g.*, Riaño *et al.*, 2004 in pine forests of central Spain) which may be integrated with SNFI data (*e.g.*, González-Ferreiro *et al.*, 2017 in pine forests of Galicia). González-Olabarría *et al.* (2012) combined fuel type derived from LiDAR data with fire behaviour models to assess fire risk at the landscape level in Urbión (Soria). At regional scale LiDAR and spectral data have been combined to provide fuel type cartography in Natural Park of Alto Tajo (Guadalajara) (García *et al.*, 2011). Likewise, to map forest fuel types in Canary Islands Marino *et al.* (2016) employed LiDAR data (1 pulse × m^{-2}) after stratification with Landsat images, and Alonso-Benito *et al.* (2016) fusioned WorldView-2 optical images and LiDAR data into an object-oriented classification approach. In the context of wildfire suppression in the wildland-urban interface, Robles *et al.* (2016) evaluated the risk of damage in case of a wildfire of buildings and infrastructures in a 36 km^2 rural area of Pontevedra. With LiDAR and aerial photographs from PNOA, and an object-oriented approach the authors classified forests into 5 forest fuel types and the buildings next to forests into 3 groups of risk.

Live fuel moisture may be estimated with passive (Chuvieco *et al.*, 2004a) or active sensors (Tanase *et al.*, 2015c), and it is an important parameter to determine fire risk, but also burning efficiency for evaluation of gas emissions from wildland fires (Chuvieco *et al.*, 2004a). Aiming to evaluate fire danger in shrubs and pastures in Cabañeros National Park, Chuvieco *et al.* (2002) employed seven Landsat images acquired at various dates—spring, summer, autumn—over three years to estimate moisture with a number of spectral indices. The authors indicated the relevance of SWIR data for estimation of vegetation moisture and interpreted spectral variations according to vegetation types. In a later work in the same area Chuvieco *et al.* (2003) employed NOAA-14 AVHRR—with low spatial resolution (1100 m) and lacking SWIR bands—images acquired during summer time in 1996-1999. A model including spectral and thermal variables was accurate (R^2 = 0.8) and helped identifying trends of moisture change in the area and when extended to other Mediterranean areas (Chuvieco *et al.*, 2004a). Comparing the performance of Landsat-TM, SPOT-Vegetation, and NOAA-AVHRR in estimation of fuel moisture, Chuvieco *et al.* (2004b) demonstrated the synergies of NIR and SWIR combined, and that the NDVI relationship with vegetation moisture over time is stronger in grasslands than in shrubs. Yebra & Chuvieco (2009) employed MODIS 8-day composites, with 500 m pixel size and including NIR

and SWIR data, to demonstrate that the retrieval of fuel moisture content is more accurate when species specific conditions are considered. The authors worked in an area dominated by *Quercus ilex* L. and compared generic and specific reflectance look-up-tables.

Despite an elusive relationship between spectral recovery and vegetation regeneration, recovery after fire is frequently studied with RS time series (*e.g.*, Vicente-Serrano, 2011; Viana-Soto *et al.*, 2017). Also with a time series approach Martínez *et al.* (2017) employed LandTrendr (Landsat-based Detection of Trends in Disturbance and Recovery, Kennedy *et al.*, 2010) an algorithm designed to characterize landscape changes, for evaluation of recovery processes in a large forest fire (> 7600 ha in Zaragoza/Navarra) characterizing patterns of spectral recovery and classes of recovery magnitude. The trajectory based approach showed there is a relationship between fire severity and recovery magnitude. Prominent among the approaches to retrieve change and regeneration information after fire is using vegetation indices such as NBR and its multi-date approach (dNBR—differential NBR, RdNBR—Relative differential NBR) (Álvarez-Taboada *et al.*, 2007b; Botella-Martínez & Fernández-Manso, 2017; Arellano *et al.*, 2017) or NDVI (Díaz-Delgado & Pons, 1999; Ruiz-Gallardo *et al.*, 2004). However, other approaches may be more informative of forest regeneration. For example, short term recovery from fire was modelled by Fernández-Manso *et al.* (2016b) in 30 km^2 of *P. pinaster* in Sierra del Teleno using a 13-year series of Landsat MESMA (Multiple Endmember Spectral Mixture Analysis) fraction images. The authors found a recovery period between 7 and 20 years depending on fire severity and indicated interpretation simplicity as an advantage of image fraction over vegetation indices time series. Tanase *et al.* (2010a) compared the sensitivity of radar (X-, C-, and L-bands) and optical data to post fire forest regrowth in various *Pinus halepensis* Mill. locations of Spain. They found that L-band backscatter is sensitive to forest structural changes 40 to 60 years past disturbance, whereas optical-based indices reach saturation within 10 to 20 years, representing a reduced monitoring capacity. LiDAR can also be useful to evaluate post-fire regeneration at the landscape level. For example, Marino *et al.* (2017b) compared metrics derived from < 4 m strata returns of three LiDAR datasets (1 pulse × m^{-2}) acquired pre- (2011) and post-fire (2012, 2014) in Garajonay and characterized vegetation recovery, demonstrating the value of repetitive LiDAR acquisitions. Debouk *et al.* (2013) employed low density LiDAR data (0.7 pulse × m^{-2}) acquired over 104 km^2 of mixed forest (*P. halepensis* and *Q. ilex*) in Barcelona five years after fire, and modelled vegetation recovery with an Artificial Neural Network (ANN) for classification and mapping. Martín-Alcón *et al.* (2015) combined low density LiDAR (0.5 pulse × m^{-2}) acquired in 2009 with MS aerial photography acquired in 2011 to classify a *P. nigra* forest burned in 1998 into five post-fire regeneration types. Malak *et al.* (2015) related vegetation regrowth over an area ~2900 km^2 in Valencia with Landsat TM EVI time series, and also demonstrated that the number of fires occurred in a short interval have a negative impact on vegetation growth. LiDAR and aerial photography combine well although both sources of data are constrained by the limited frequency of acquisition. Regeneration after a large fire has been recently studied with ultra-high spatial resolution imagery (0.2 m) acquired with UAV technology during a two-month campaign (Fernández-Guisuraga *et al.*, 2018) in a 3000 ha area in León. Despite some banding noise and non-homogeneous radiometry, when compared with high spatial resolution WorldView-2 data (2 m pixel size) the UAV provided more accurate information of structural variability.

Health status

The Spanish forests and plantations host endemic populations of insects like the pine processionary moth (*Thaumetopoea pityocampa* D. &. Schiff.), the European gypsy moth (*Lymantria dispar* L.), the beech weevil (*Rhynchaenus fagi* L.) or the eucalyptus snout beetle (*Gonipterus platensis* Marelli). These populations cause low level defoliations but eventual outbreaks may occur in years of climate deviations (Cardil *et al.*, 2017). Monitoring is necessary to evaluate the severity and areal extent of pest effects on the health and growth of trees, for management, and to develop effective protection strategies. The Spanish national forest health monitoring system is based on field observations over a network of plots (UNECE, 2016) and provides valuable data for overall assessments, but has inherent limitations for detailed mapping. RS data with complete spatial coverage and periodical observations may enhance the value of in situ measurements, and facilitate modelling and assessment of trends and deviations from normal condition. However, according to Radeloff *et al.* (1999) monitoring defoliation with RS is hampered by three problems: the short periods when defoliation can be detected, a difference in the scale of affection (leaves) and detection (canopy), and the close interactions between factors and effects on insect populations.

Discerning the canopy reflectance signal from noise in forests slightly affected by a pest or disease requires fine spatial and spectral resolutions coupled with the

right temporal acquisitions, ideally at pre-, peak-, and post-defoliation times (Rullán *et al.*, 2013). Rullán *et al.* (2013) suggested a two level scaled system for regional or national level monitoring of insect defoliation, with an early warning provided by MODIS time series, and Landsat data to assess damage affection. In 2004 Álvarez-Taboada *et al.* proposed a monitoring system of the health status in *Eucalyptus globulus* Labill. incorporating modelling, RS, and GIS (Eucalyptus Health Monitoring System, EHMS). Although an optimal application of the EHMS depends on climatic, soil and forest stand data, and validation of some relationships between the radiometric information and eucalyptus stand parameters, damage detection just requires Landsat TM SWIR data, a DEM, and stand density data. When applied in Galicia the EHMS identified damaged stands with leaf loss over 25% with a true positive accuracy of 72.31% and user's accuracy of 95.92% (Álvarez-Taboada, 2006; Álvarez-Taboada *et al.*, 2007a). SAR-based change detection approaches may be better suited to identify areas susceptible to insect outbreaks or experiencing the initial outbreak phase, as demonstrated for coniferous forests elsewhere (Tanase *et al.*, 2018). In this work the L-band SAR backscatter was sensitive to insect induced changes a year in advance when compared to optical reflectance from high resolution orthophotos. Such differences were explained by the sensitivity of the SAR data to the vegetation moisture content, which decreases during the initial attack phase (green phase) when leaves are still green (*i.e.*, there is little to no change in optical reflectance).

As noted by Carter (1993) discoloured vegetation stressed by a pest or disease increases reflectance in the green and red (VIS), an effect typically first observed in the red edge (0.7 μm), whereas defoliation is identifiable by a decrease in the NIR reflectance (Jensen, 2005). Vegetation indices based on VIS, NIR, and SWIR wavelengths are frequently used to quantify forest defoliation. In particular the ratio between SWIR and NIR, named Moisture Stress Index (MSI, Rock *et al.*, 1986) has been found to be strongly related with defoliation caused by diverse drivers (*e.g.*, pine processionary moth in Sierra de Gúdar (Teruel)—Sangüesa-Barreda *et al.* (2014); beech weevil in the southern Cantabrian range—Rullán-Silva *et al.*, 2015). In absence of extreme defoliation, modelling damage with MSI becomes more robust for intervals of low and moderate affection (Rullán-Silva *et al.*, 2015). Álvarez-Taboada *et al.* (2014) developed a multi-sensor and multi-scale system for monitoring forest health in *P. radiata* stands affected by the European gypsy moth in a study area of 150 ha in Cubillos del Sil, León. At stand level the authors identified three levels of defoliation severity employing pre- and post- outbreak Landsat OLI data and an object oriented supervised approach, achieving an overall accuracy of 97.61%. In the same area Castedo Dorado *et al.* (2016) tested the UAV technology with RGB and NIR images (Ground Sample Distance, GSD = 0.15 m) acquired with a fixed-wing platform to map defoliation severity at tree level. Overall accuracies were 67.68%, 71.72%, and 92.93% for 4, 3, and 2 severity classes. Also using UAVs Cardil *et al.* (2017) assessed defoliation by the pine processionary moth in two pine stands in an area of 24.6 ha. The authors classified RGB images captured with a Phantom 3 DJI and validated the results with field estimations at the tree level. The accuracy of detection was 79%, and only a few trees with low level of defoliation (10-20%) were misclassified.

Pests and diseases may have long term effects on trees that are more difficult to notice with RS than temporal defoliation, requiring additional data for interpretation. Sangüesa-Barreda *et al.* (2014) combined Landsat data with dendrochronological characterization of changes in basal area to estimate loss of growth due to the processionary moth. Cifuentes *et al.* (2017) classified affections caused by the fungus *Cryphonectria parasitica* (Murrill) (blight) in chestnut stands in El Bierzo (León). The authors estimated blight severity levels by visual analysis of RGB ortophotography (GSD = 0.08 m) acquired with a fixed-wing UAV and validated its correspondence to 182 field measurements. The overall accuracy for six severity levels was 63%, whereas for 5and 4 levels, was 74% and 77%, showing usefulness of this approach to map blight severity at the tree level.

For an early detection of forest decline photosynthetic activity and pigment content are better indicators than structural degradation. Sun induced fluorescence (SIF), which can be assessed from ultraviolet active laser fluorosensors and from passive multispectral or hyperspectral radiance sensors, has shown to be a proxy of photosynthetic activity. *Q. ilex* declining condition due to water stress and *Phytophtora* was explored by Hernández-Clemente *et al.* (2017) analysing the red and far-red SIF from airborne hyperspectral imagery. The authors found the relationships between SIF and vigour decline depend on spatial resolution, being significant for 0.6 m pixels but not for 30 m pixels. Recently Zarco-Tejada *et al.* (2018) explored the capacity of red-edge spectral data to assess pine decline in 7000 ha of *P. pinaster* and *P. nigra* in Extremadura analysing the temporal responses of Sentinel-2A red edge chlorophyll index and NDVI. Validated with aerial hyperspectral data and field measures of chlorotic and defoliated trees the authors found that declining and healthy pine trees have different NDVI vs. chlorophyll

index temporal trajectories, demonstrating the value of the red-edge data to monitor forest decline.

Synthesis

Forests and other woodlands cover more than half of the Spanish land and provide important services to society, including economic benefits and recreational opportunities. RS offers options for monitoring the environment and it is increasingly being employed to improve our understanding on the state and dynamics of forest ecosystems in Spain. Applications that benefit from the use of RS techniques include medium to large scale characterization of forest structure, estimation of aboveground biomass, mapping of fire extension and severity, and monitoring of forest health. Certainly optical medium spatial resolution data have been the most frequently used source of data in the past, due to availability and suitability for a range of applications. However, LiDAR and SAR data are increasingly being employed (Table 3), especially for the retrieval of forest structural parameters, due to their capability to penetrate through the canopy. Innovative RS techniques are developed and applied in Spanish forests, being remarkable the use of small aerial platforms (UAVs) for local scale data acquisition and assisting in assessment of forest health, and the application of machine learning for analysis and modelling.

Through this review we have identified some needs and opportunities in the monitoring of Spanish forests where RS techniques can play a significant role (Table 5). In general free access to abundant and frequent data, as well as the increased storing and processing capacity offer unprecedented opportunities for forestry RS applications at spatial scales from local to national and with detailed temporal recurrence. Extending local models to a national level to provide an overall and consistent perspective should be a pursued effort, and understanding dynamics retrospectively would provide baseline information to build knowledge for the future. In this review we mentioned a representation of the most relevant RS applications in Spanish forests found in the scientific literature, with special attention to the most recent ones.

Transversal to landscape, structure, fire, and health is the dynamic character of ecosystems. Perhaps the most remarkable current opportunity offered by RS technology resides in its capacity to characterize dynamics at a range of temporal resolutions, facilitated by the amount of free data available from long-life duration satellites like Landsat, MODIS and the Sentinels. There is an opportunity to monitor trends with high temporal frequency and spatial resolution and to retrospectively reconstruct a history of change to learn from patterns, by combining the Landsat records held by the USGS and ESA archives. Integration of data from both archives requires self-implemented standard processing

Table 5. Synthesis of the needs and opportunities in the Spanish forestry remote sensing

NEED	OPPORTUNITY	TECHNIQUE
Frequent LULC	Sentinel-2 Sentinel-1 Virtual constellations	Integration of synergic data Classification
Historical fire cartography	Landsat Combine USGS and ESA image archives	Standardized pre-processing Spectral trend analysis
Fire risk	MODIS Landsat Sentinel-2	Hot-spots Deviation from time series
Fire behaviour and propagation	SWIR imagery LiDAR discrete and full-waveform	Modelling
Structural characterization	LiDAR DAP point clouds Radar	Combined and synergic use of LiDAR and DAP Polarimetry PolInSAR
Height characterization	LiDAR	Standard processing extended to large scale
Height change assessment	Radar data from Tandem X/PAZ LiDAR / DAP point clouds	PolInSAR Combined and synergic use of LiDAR and DAP
Health assessment	Sentinel-1/2 UAV	Time series Calibration and assessment at local scale
Characterization of forest dynamics	Virtual constellations (Sentinel -1/2, Landsat)	Time series Modelling
Habitat cartography	Combination of moderate resolution with UAV data	Two scale monitoring

(*i.e.*, geometric alignment and radiometric corrections) until the Landsat Global Archive Consolidation initiative (Wulder *et al.*, 2016) completes efforts to have all images centralized in a global archive and with similar processing. To overcome eventual scarcity of available data due to historical circumstances, compositing data with a per-pixel approach (White *et al.*, 2014) facilitates complete coverage with high frequency. Hence, phenological characterization of forest ecosystems (Pasquarella *et al.*, 2016; Simonson *et al.*, 2018) and identification of species for habitat mapping or characterization of invasive species after fire (Bradley, 2014) are enabled, adding insights to our understanding of global change. The need to understand changes in species dominance and structural dynamics retrospectively, as well as recovery after fire, exists in Spain for reporting and management at national scale. Linking historical records and current insights facilitates prospective modelling in different scenarios for informed decisions.

National scale landscape characterization currently based on SIOSE, CORINE, and MFE products may be improved with more frequent land cover updates. For example, incorporating data from the European Copernicus Programme—optical Sentinel-2 and radar Sentinel-1—and data from the Landsat Programme may update LC products and enable monitoring changes annually (Gómez *et al.*, 2016b; Hermosilla *et al.*, 2016; Hermosilla *et al.*, 2018). Trade-offs between temporal frequency and spatial or spectral resolutions in data acquisition have reduced their relevance thanks to virtual constellations (Wulder *et al.*, 2015) that provide a stream of available and compatible data from different satellite programs. For retrospective monitoring of landscape dynamics Landsat is undoubtedly the most adequate source of data, due to its long–term archive, spatial resolution, and spectral quality. Retrospectively identifying changes at large scale with a time series approach (*e.g.*, C2C, LandTrendr) and interpreting rates of change (*e.g.*, Gómez *et al.*, 2012a) helps understanding patterns as well as drivers of change (Regos *et al.*, 2015).

For an accurate assessment of resources at national level, forest structural maps including height, canopy cover, and biomass will benefit overall reports, management, and habitat mapping. At regional or national scale characterizing structure with RS requires extensive and reliable continuous data, and there are currently a range of opportunities. Although single-date optical data has typically yielded models with high relative errors, seasonal imagery acquired at key dates over the year have demonstrated higher accuracy in estimation of tree density, basal area, and wood volume in Mediterranean forests (Chrysafis *et al.*, 2017). Undoubtedly the national coverage of PNOA LiDAR data provides a unique opportunity to create a national map of forest structure. With a sampling approach PNOA LiDAR can also be used to calibrate predictive models of forest structure metrics and biomass using optical time series data, an effort successfully implemented at very large scale in Canada (*e.g.*, Zald *et al.*, 2016). Additionally, a second complete coverage acquisition of LiDAR data with comparable density and precision will facilitate structural comparisons over time and assessment of change. However, for a reliable characterization of all kinds of forest structure, it would be beneficial to attain an increase in the scanning density of the national level PNOA LiDAR data (Adnan *et al.*, 2017). Higher point densities would also facilitate the implementation of individual tree methods (*e.g.*, Valbuena-Rabadán *et al.*, 2016). In order to enable the production of updated results PNOA LiDAR data has to be promptly available to users. Combining LiDAR and photogrammetric data might be a cost effective option for regular assessment of change in forest structure (Tompalski *et al.*, 2018; Navarro *et al.*, 2018). With increased temporal frequency, the demonstrated synergies between LiDAR and optical data for large area mapping of structure (Manzanera *et al.*, 2016; Matasci *et al.*, 2018) could provide relevant results in Spain, at least in the most dynamic areas. At detailed scales, species identification and structural analysis at tree level are possible by combining multispectral images and LiDAR data (*e.g.*, González-Ferreiro *et al.*, 2013b), and in the near future multispectral LiDAR will provide an integrated alternative. Radar data has capacity to characterize forest height and height change applying interferometric (Olesk *et al.*, 2016) and Pol-Insar techniques (Xie *et al.*, 2017) over large regions like the Spanish national territory. PolInsar metrics make feasible the retrieval of information on the vertical structure of forests which may overcome saturation effects when estimating biomass or height (López-Sánchez & Ballester-Berman, 2009). Data from the TanDEM-X mission are available for research (Table 1) and data from the Spanish PAZ launched in 2018 will be fully compatible with Tan DEM-X, adding to the stream of data. Sentinel-1, although not optimally configured in polarization and frequency for forestry applications, offers a large amount of frequent data and opportunities still unexplored. Satellite radar missions like BIOMASS, expected to orbit in the near future, and satellite constellations combining multiple sensors may open important opportunities to monitor forest resources. Playing a key role for calibration and verification, UAVs equipped with one or more sensors already enhance the characterization of forest

structure (*e.g.*, Sankey *et al.*, 2017). And in the future, unmanned high altitude platforms or pseudo-satellites (HAPS) flying at around 20 km height, will provide a link between data acquisition scales, complementing satellite and aircraft imagery (Gonzalo *et al.*, 2017).

Driven by the relevance of fire as trigger of change in Spanish forests, a great effort was focused in the last decades on fire related RS applications. Still, complete and updated national scale cartographic records of fire at high spatial resolution are missing, and most assessments rely on non-spatially explicit statistics. Developing historical annual cartography of fire in forest areas with high accuracy is feasible with the current availability of data (Gómez *et al.*, 2017), facilitating analysis and interpretation of change patterns and drivers of change (Cohen *et al.*, 2016; White *et al.*, 2017). As a modelling technique the mapping limitations should be reported to avoid misinterpretation or overstating results, providing measures of accuracy and confidence intervals. As the archive of available data gets longer, standardizing data quality to apply novel algorithms is possible (*e.g.*, Hermosilla *et al.*, 2017) and enables the maintenance of maps up to date. Moreover, identification of hot spots and characterization of the wildland urban interface at different scales for operational use in wildfire prevention and suppression, and planning of prescribed fires benefit from the use of time series of Landsat OLI and Sentinel-2 as well as LiDAR data. SAR-based burned area detection algorithms are also developed under the ESA Fire-CCI Phase 2 project (Lohberger *et al.*, 2018; Belenguer-Plomer *et al.*, 2018) and may be applied at national scale. Also relevant for fire management is the capacity of radar data to estimate live fuel under forest canopy demonstrated by Tanase *et al.* (2015c). LiDAR data can be used to estimate fuel variables of the forest canopy, crucial information used as input in fire behaviour models, while full-waveform systems are proper to provide information of the understory vegetation (Crespo-Peremarch *et al.*, 2018), particularly relevant in Mediterranean ecosystems where shrubs are main drivers of wildfire regime. Future attention should be paid to LiDAR satellites, such as IceSAT-2 and GEDI, possibly coupled with TanDEM-X, since these data will become available from 2019. These new sensors will likely open a new range of operational and research applications.

Biological invasions, pests, and diseases progressively getting more frequent and intense may compromise the health of Spanish forests. To meet the operational needs of timely and accurate forest health monitoring systems nowadays efforts focus on integrating data at various scales. Comprehensive and spatially-explicit data—only feasible from RS—contribute towards increasing our knowledge of the invasions biology and developing more efficient management strategies (Hernández *et al.*, 2014; Pascual *et al.*, 2016). RS techniques also improve the efficiency of sampling for prediction of outbreaks (Wulder & Dymond, 2004). In this sense UAV technologies have emerged as an opportunity offering above canopy perspective of stand condition that can bridge field to satellite scales, and as a source of data for calibration and validation of RS monitoring systems (Hall *et al.*, 2016). Two of the major threats to the chestnut stands in Spain are *Cryphonectria parasitica* (chestnut blight) and *Phytophthora cinnamomi* (ink disease) (Melicharová & Vizoso-Arribe, 2012), which eventually can cause the death of trees. Combining data from different sensors mounted on UAVs can provide helpful information (*e.g.*, detection, monitoring of the treatments) about infestations which require treatments at tree or at stand level. Detecting and monitoring *Bursaphelenchus xylophilus* (a pine wood nematode), and *Xylella fastidiosa*, the biggest hazards regarding forest health in Spain (Karnkowski & Sahajdak, 2010) remains challenging. *Xylella fastidiosa* is one of the most dangerous plant bacteria worldwide, causing a variety of diseases with huge economic impact (Sherald, 2007). Due to its severity and economic impact, the European Union has taken emergency control measures for both (EC, 2017), which involves their detection, location, and monitoring. For an early detection with RS high spatial and hyperspectral imagery is needed, being multispectral imagery useful to supervise and monitor whether the affected stands have been removed, and whether the decay is spreading beyond the demarcated areas. Despite the ephemeral character of defoliation, near real time monitoring of this effect is possible with dense time series of multispectral data (Pasquarella *et al.*, 2017) at stand or forest scale, although the defoliation driver may remain unknown. Common pests in forest plantations like defoliators of *Eucalyptus* spp. (*e.g.*, *Gonipterus platensis*) or pine engravers like the bark beetle (*Ips sexdentatus*) which causes decay and even death of *Pinus spp*. may be monitored in Spain with this approach. Especially in the case of the bark beetle, monitoring the decay will help knowing whether the population is under control or whether pheromone traps or tree removal is needed to prevent its spread. A quick spread of new pests like the chestnut gall wasp (*Dryocosmus kuriphilus*) is an outstanding example of recent human-aided biological invasion with ecological impacts and economic losses (Bonal *et al.*, 2018). Detecting this type of pest with RS is challenging unless the level of infestation is very high, but in heavily infested areas monitoring the treatment success at stand level could be a suitable task

for multispectral high spatial resolution imagery (*e.g.*, Sentinel-2, World View-4).

Overall, RS contributes to our better understanding of the services provided by Spanish forest ecosystems, allowing insights on the forest state and dynamics and this helping towards a better planning and sustainable management. We live a time of opportunities provided by the use of optical, radar, hyperspectral or LiDAR sensors, individually or in combinations that leverage their synergies for forestry applications.

Acknowledgments

We thank the reviewers and editor for their thorough work and contributions to the final manuscript version.

References

Adnan S, Maltamo M, Coomes DA, Valbuena R, 2017. Effects of Plot Size, Stand Density and Scan Density on the Relationship between Airborne Laser Scanning Metrics and the Gini Coefficient of Tree Size Inequality. Can J Forest Res 47 (12): 1590-1602. https://doi.org/10.1139/cjfr-2017-0084

Adnan S, Maltamo M, Coomes DA, García-Abril A, Malhi Y, Manzanera JA, Butt N, Morecroft M, Valbuena R, 2018. A simple approach to forest structure classification using airborne laser scanning that can be adopted across bioregions. Forest EcolManag 433: 111-121. https://doi.org/10.1016/j.foreco.2018.10.057

Alberdi I, Vallejo R, Álvarez-González JG, Condés S, González-Ferreiro E, Guerrero S, Hernández L, Martínez-Jáuregui M, Montes F, Oliveira N, *et al.*, 2017. The multi-objective Spanish National Forest Inventory. Forest Syst 26 (2): e04S. https://doi.org/10.5424/fs/2017262-10577

Alonso-Benito A, Arroyo LA, Arbelo M, Hernández-Leal P, 2016. Fusion of WorldView-2 and LiDAR data to map fuel types in the Canary Islands. RemoteSens-Basel 8 (8): 669. https://doi.org/10.3390/rs8080669

Álvarez-Martínez JM, Jiménez-Alfaro B, Barquín J, Ondiviela B, Recio M, Silió-Calzada A, Juanes JA, 2017. Modelling the area of occupancy of habitat types with remote sensing. MethodsEcolEvol 9: 580-593. https://doi.org/10.1111/2041-210X.12925

Álvarez-Taboada MF, Cimadevila HL, Rodríguez Pérez JR, Picos Martín J, 2004. Workflow to improve the forest management of Eucalyptus globulus stands affected by Gonipterusscutellatus in Galicia, Spain using remote sensing and GIS, Proc. SPIE 5574, Remote Sensing for Environmental Monitoring, GIS Applications, and Geology IV, (22 October 2004).

Álvarez-Taboada MF, 2006. Remote sensing and Geoinformation systems applied to the forest management of Eucalyptus globulusLabill. Stands damaged by GonipterusscutellatusGyllendall in Galicia. Doctoral Thesis. Universidade de Vigo. 319 pp.

Álvarez-Taboada MF, Lorenzo Cimadevila H, Wulder M, 2007a. Monitorización del estado sanitario de las masas de Eucapyptusglobulus en Galicia empleando modelos de proceso, SIG y teledetección. Proc 2º simposio iberoamericano de Eucalipto Globulus in Vigo (Spain). October 17-20, CIDEU 4 vol II, pp 41-47.

Álvarez-Taboada MF, Rodríguez-Pérez JR, Castedo-Dorado F, Vega-Nieva D, 2007b. An operational protocol for post-fire evaluation at landscape scale in an object-oriented environment. Proceedings of the 6th International Workshop of the EARSeL Special Interest Group on Forest Fires JRC 8072. pp 202 – 207 (2007). 6th International Workshop of the EARSeL Special Interest Group on Forest Fires. Tesalonica, Grecia.

Álvarez-Taboada, F, Sanz-Ablanedo, E, Rodríguez Pérez, JR, Castedo-Dorado F, Lombardero MJ, 2014. Multi-sensor and multi-scale system for monitoring forest health in Pinusradiata stands defoliated by Lymantriadispar in NW Spain. Proceedings of the ForestSAT Open Conference System, http://ocs.agr.unifi.it/index.php/forestsat2014/ForestSAT2014/paper/view/245

Aragonés D, Rodríguez-Galiano V, Caparros-Santiago JA, Navarro-Cerrillo RM, 2017. El uso de la fenología de la superficie terrestre para discriminar entre especies de pinos mediterráneos. Nuevas plataformas y sensores de teledetección, XVII Congreso de la Asociación Española de Teledetección (Eds. Ruiz LA, Estornell J, Erena M), Murcia (Spain), October 3-7, pp: 219-222.

Arellano S, Vega JA, Rodríguez y Silva F, Fernández C, Vega-Nieva D, Álvarez-González JG, Ruiz-González AD, 2017. Validación de los índices de teledetección dNBR y RdNBR para determinar la severidad del fuego en el incendio forestal de Oia-O Rosal (Pontevedra) en 2013. Revista de Teledetección 49: 49-61. https://doi.org/10.4995/raet.2017.7137

Arellano-Pérez S, Castedo-Dorado F, López-Sánchez C, González-Ferreiro E, Yang Z, Díaz-Varela R, Ruiz-González A, 2018. Potential of Sentinel-2A Data to Model Surface and Canopy Fuel Characteristics in Relation to Crown Fire Hazard. RemoteSens-Basel 10(10): 1645. https://doi.org/10.3390/rs10101645

Arias-Rodil M, Diéguez-Aranda U, Álvarez-González JG, Pérez-Cruzado C, Castedo-Dorado F, González-Ferreiro E, 2018. Modeling diameter distributions in radiata pine plantations in Spain with existing countrywide LiDAR data. Ann ForSci 75 (2): 1-12.

Arozarena A, Villa G, Hermosilla J, Papí F, Valcárcel N, Peces JJ, Doménech E, García C, Tejeiro JA, 2006. El Plan Nacional de Observación del Territorio en Espa-a:

situación actual y próximos pasos. Mapping Interactivo 111: 16-22.

Arroyo LA, Healey SP, Cohen WB, Cocero D, Manzanera JA, 2006. Using object-oriented classification and high-resolution imagery to map fuel types in a Mediterranean region. J Geophys Res 111: G04S04. https://doi.org/10.1029/2005JG000120

Askne JIH, Santoro M, Smith G, Fransson JES, 2003. Multitemporal Repeat-Pass SAR Interferometry of Boreal Forests. IEEE Trans Geosci Rem Sens 41: 1540-1550. https://doi.org/10.1109/TGRS.2003.813397

Aulló-Maestro I, Gómez C, Cuevas R, Rubio A, Montes F, 2017. Dinámica forestal de Pinussylvestris L. y Quercus pyrenaica Willd. en el bosque de Hoyocasero (Ávila) mediante serie temporal Landsat (1984-2016) y métodos geoestadísticos. Nuevas plataformas y sensores de teledetección, XVII Congreso de la Asociación Española de Teledetección (Eds. Ruiz LA, Estornell J, Erena M), Murcia (Spain), October 3-7, pp: 143-146.

Axelsson C, Skidmore AK, Schlerf M, Fauzi A, Verhoef W, 2012. Hyperspectral analysis of mangrove foliar chemistry using PLSR and support vector regression. Int J Remote Sens 34: 1724-1743. https://doi.org/10.1080/01431161.2012.725958

Banskota A, Kayastha N, Falkowski MJ, Wulder MA, Froese RE, White JC, 2014. Forest Monitoring Using Landsat Time Series Data: A Review. Can J Remote Sens 40: 362-384. https://doi.org/10.1080/07038992.2014.987376

Bastarrika A, Alvarado M, Artano K, Martínez MP, MesanzaA, Torre L, Ramo R, Chuvieco E, 2014. BAMS: A Tool for Supervised Burned Area Mapping Using Landsat Data. RemoteSens-Basel 6: 12360-12380. https://doi.org/10.3390/rs61212360

Belenguer-Plomer MA, Tanase MA, Fernández-Carrillo A, Chuvieco E, 2018. Insights into burned areas detection from Sentinel-1 data and locally adaptive algorithms, Proc. SPIE 10790, Earth Resources and Environmental Remote Sensing/GIS Applications IX, 107901S (9 October 2018).

Belward AS, Skøien JO, 2015. Who launched what, when and why; trends in global land-cover observation capacity from civilian earth observation satellites. ISPRS J Photogramm103: 115-128.

Bengoa JL, De Blanco V, Nafria DA, 2017. Clasificación semiautomática de cubiertas naturales arboladas en Castilla y León. 7º Congreso Forestal Español. 26-30 de junio de 2017. Plasencia, Cáceres, España.

Blanco-Martínez J, Rodríguez F, Martínez S, Martínez AA, García JB, Fernández JJ, Roldán A, Diez FJ, Lizarralde I, Cabrera M, 2017. Generación de un inventario forestal regional y una cartografía de modelos de combustible para Castilla-La Mancha. 7 Congreso Forestal Español, 26-30 de junio, Plasencia, Spain.

Blázquez-Casado Á, González-Olabarria JR, Martín-Alcón S, Just A, Cabré M, Coll Ll, 2015. Assessing post-storm forest dynamics in the Pyrenees using high-resolution LiDAR data and aerial photographs. J Mt Sci 12 (4): 841. https://doi.org/10.1007/s11629-014-3327-3

Bonal R, Vargas-Osuna E, Mena JD, Aparicio JM, Santoro M, Martín A, 2018. Looking for variable molecular markers in the chestnut gall wasp Dryocosmus kuriphilus: First comparison across genes Scientific Reports. 8. 10.1038/s41598-018-23754-z. https://doi.org/10.1038/s41598-018-23754-z

Borràs J, Delegido J, Pezzola A, Pereira M, Morassi G, Camps-Valls G, 2017. Clasificación de usos del suelo a partir de imágenes Sentinel-2. Revista de Teledetección 48: 55-66. https://doi.org/10.4995/raet.2017.7133

Botella-Martínez MA, Fernández-Manso A, 2017. Estudio de la severidad post-incendio en la Comunidad Valenciana comparando los índices dNBR, RdNBR y RBR a partir de imágenes Landsat 8. Revista de Teledetección 49: 33-47. https://doi.org/10.4995/raet.2017.7095

Bottalico F, Chirici G, Giannini R, Mele S, Mura M, Puxeddu M, McRoberts RE, Valbuena R, Travaglini D, 2017. Modeling Mediterranean Forest Structure Using Airborne Laser Scanning Data. Int J Appl Earth Obs 57: 145-153. https://doi.org/10.1016/j.jag.2016.12.013

Bradley BA, 2014. Remote Detection of Invasive Plants: A Review of Spectral, Textural and Phenological Approaches. BiolInvasions 16: 1411-1425. https://doi.org/10.1007/s10530-013-0578-9

Cabello J, Alcaraz-Segura D, Reyes A, Lourenço P, Requena JM, Bonache J, Castillo P, Valencia S, Naya J, Ramírez L, Serrada J, 2016. Sistema para el seguimiento del funcionamiento de ecosistemas en la Red de Parques Nacionales de España mediante teledetección. Revista de Teledetección 46: 119-131. https://doi.org/10.4995/raet.2016.5731

Camarero JJ, Bigler C, Linares JC, Gil-Pelegrín E, 2011. Synergistic effects of past historical logging and drought on the decline of Pyrenean silver fir forests. For Ecol Manage 262: 759–769.

Cardil A, Vepakomma U, BrotonsLl, 2017. Assessing processionary moth defoliation using unmanned aerial systems. Forests 8: 402. https://doi.org/10.3390/f8100402

Carter G, 1993. Responses of leaf spectral reflectance to plant stress. Am J Bot 80: 231-243. https://doi.org/10.1002/j.1537-2197.1993.tb13796.x

Cartus O, Santoro, M., Kellndorfer J, 2012. Mapping forest aboveground biomass in the Northeastern United States with ALOS PALSAR dual-polarization L-band. Remote Sens Environ 124: 466-478. https://doi.org/10.1016/j.rse.2012.05.029

Castedo-Dorado F, Lago-Parra G, Lombardero MJ, Liebhold AM, Álvarez-Taboada F, 2016. European gypsy moth (Lymantriadispardispar L.) completes development and defoliates exotic radiata pine plantations in Spain. New Zeal J ForSci 46: 18. https://doi.org/10.1186/s40490-016-0074-y

Chrysafis I, Mallinis G, Gitas I, Tsakiri-Strati M, 2017. Estimating Mediterranean forest parameters using multi seasonal Landsat 8 OLI imagery and an ensemble learning method. Remote Sens Environ 199: 154-166. https://doi.org/10.1016/j.rse.2017.07.018

Chuvieco E, Riaño D, Aguado I, Cocero D, 2002. Estimation of fuel moisture content from multitemporal analysis of Landsat Thematic Mapper reflectance data: applications in fire danger assessment. Int J RemoteSens 23 (11): 2145-2162. https://doi.org/10.1080/01431160110069818

Chuvieco E, Aguado I, Cocero D, Riaño D, 2003. Design of an empirical index to estimate fuel moisture content from NOAA–AVHRR analysis in forest fire danger studies. Int J RemoteSens 24(8): 1621-1637. https://doi.org/10.1080/01431160210144660b

Chuvieco E, Cocero D, Riaño D, Martínez P, Martínez-Vega J, De la Riva J, Pérez F, 2004a. Combining NDVI and surface temperature for the estimation of live fuel moisture content in forest fire danger rating. Remote Sens Environ 92: 322-331. https://doi.org/10.1016/j.rse.2004.01.019

Chuvieco E, Cocero D, Aguado I, Palacios-Orueta A, Prado E, 2004b. Improving burning efficiency estimates through satellite assessment of fuel moisture content. J Geoph Res-Atmos 109: D14S07.

Chuvieco E, De Santis A, Riaño D, Halligan K, 2007. Simulation approaches for burn severity estimation using remotely sensed images. Fire Eco 3 (1): 129-150. https://doi.org/10.4996/fireecology.0301129

Cicuéndez V, Litago J, Huesca M, Rodríguez-Rastrero M, Recuero L, Merino de Miguel S, Palacios-Orueta A, 2015. Assessment of the gross primary production dynamics of a Mediterranean holm oak forest by remote sensing time series analysis. AgroforestSyst 89 (3): 491-510. https://doi.org/10.1007/s10457-015-9786-x

Cifuentes JM, Fernández-Manso A, Sanz-Ablanedo E, 2017. Utilización de vehículo aéreo no tripulado (VANT) en el estudio de los niveles de severidad por chancro del castaño en el NO de España. In: Nuevas plataformas y sensores de teledetección. Nuevas plataformas y sensores de teledetección, XVII Congreso de la Asociación Española de Teledetección (Eds. Ruiz LA, Estornell J, Erena M), Murcia (Spain), October 3-7, pp: 477-480.

Clark ML, Roberts DA, Clark DB, 2005. Hyperspectral discrimination of tropical rain forest tree species at leaf to crown scales. Remote Sens Environ 96: 375-398. https://doi.org/10.1016/j.rse.2005.03.009

Claverie M, Ju J, Masek JG, Dungan JL, Vermote EF, Roger J-C, Skakun SV, Justice C, 2018. The harmonized Landsat and Sentinel-2 surface reflectance data set. Remote Sens Environ 219: 145-161. https://doi.org/10.1016/j.rse.2018.09.002

Cloude SR, Papathanassiou KP, 1998. Polarimetric SAR Interferometry. IEEE Trans Geosci Rem Sens 36: 1551-1565. https://doi.org/10.1109/36.718859

Cohen WB, Goward SN, 2004. Landsat's role in ecological applications of remote sensing. Biosciences 54 (6): 535-545. https://doi.org/10.1641/0006-3568(2004)054[0535:LRIEAO]2.0.CO;2

Cohen WB, Yang Z, Stehman SV, Schroeder TA, Bell DM, Masek JG, Huang Ch, Meighs GW, 2016. Forest disturbance across the conterminous United States from 1985-2012: the emerging dominance of forest decline. Forest EcolManag 360: 242-252. https://doi.org/10.1016/j.foreco.2015.10.042

Cohen WB, Yang Z, Healey SP, Kennedy RE, Gorelick N, 2018. A LandTrendr multispectral ensemble for forest disturbance detection. Remote Sens Environ 205: 131-140. https://doi.org/10.1016/j.rse.2017.11.015

Condés S, Fernández-Landa A, Rodríguez F, 2013. Influencia del inventario de campo en el error de muestreo obtenido en un inventario con tecnología LiDAR. 6° Congreso Forestal Español. SECF

Crespo-Peremarch P, Tompalski P, Coops NC, Ruiz LA, 2018. Characterizing understory vegetation in Mediterranean forests using full-waveform airborne laser scanning data. Remote Sens Environ 217: 400-413. https://doi.org/10.1016/j.rse.2018.08.033

Cubbage F, Harou P, Sills E, 2007. Policy instruments to enhance multi-functional forest management. Forest Policy Econ 9: 833-851. https://doi.org/10.1016/j.forpol.2006.03.010

Datt B, McVicar TR, Van Niel TG, Jupp DLB, Pearlman JS, 2003. PreprocessingEO-1 Hyperion hyperspectral data to support the application of agricultural indexes. IEEE T GeosciRemote 41: 1246-1259. https://doi.org/10.1109/TGRS.2003.813206

De Santis A, Chuvieco E, 2007. Burn severity estimation from remotely sensed data: performance of simulation versus empirical models. Remote Sens Environ 108: 422-435. https://doi.org/10.1016/j.rse.2006.11.022

De Santis A, Chuvieco E, 2009. GeoCBI: A modified version of the Composite Burn Index for the initial assessment of the short-term burn severity from remotely sensed data. Remote Sens Environ 113: 554-562. https://doi.org/10.1016/j.rse.2008.10.011

Debouk H, Riera-Tatche R, Vega-García C, 2013. Assessing Post-Fire Regeneration in a Mediterranean Mixed Forest Using LiDAR Data and Artificial Neural Networks. 2013. PhotogrammEng Rem S 79 (12): 1121-1130. https://doi.org/10.14358/PERS.79.12.1121

Diaz-Balteiro L, Romero C, 2008. Making forestry decisions with multiple criteria: A review and an assessment. Forest EcolManag 255: 3222-3241. https://doi.org/10.1016/j.foreco.2008.01.038

Díaz-Delgado R, Pons X, 1999. Empleo de imágenes de teledetección para el análisis de los niveles de severidad causados por el fuego. Revista de Teledetección 12: 63-68.

Dobson MC, Ulaby T, Le Toan T, Beaudoin A, Kasischke ES, 1992. Dependence of radar backscatter on coniferous

forest biomass. IEEE Trans Geosci Rem Sens 30: 412-415. https://doi.org/10.1109/36.134090

Domingo D, Lamelas-Gracia MT, Montealegre-Gracia AL, de la Riva-Fernández J, 2017. Comparison of regression models to estimate biomass losses and CO2 emissions using low-density airborne laser scanning data in a burnt Aleppo pine forest. Eur J RemoteSens 50 (1): 384-396. https://doi.org/10.1080/22797254.2017.1336067

Domingo D, Lamelas M, Montealegre A, de la Riva J, 2018. Estimation of Total Biomass in Aleppo Pine Forest Stands Applying Parametric and Nonparametric Methods to Low-Density Airborne Laser Scanning Data. Forests 9 (4): 158. https://doi.org/10.3390/f9040158

Duncanson LI, Neimann KO, Wulder MA, 2010. Integration of GLAS and Landsat TM data for aboveground biomass estimation. Can J RemoteSens 36 (2): 129-141. https://doi.org/10.5589/m10-037

Estornell J, Ruiz LA, Velázquez-Martí B, Fernández-Sarría A, 2011a. Estimation of shrub biomass by airborne LiDAR data in small forest stands. Forest EcolManag 262: 1697-1703. https://doi.org/10.1016/j.foreco.2011.07.026

Estornell J, Ruiz LA, Velázquez-Marti B, 2011b. Study of shrub cover and height using LiDAR data in a Mediterranean area. ForSci 57 (3): 171-179.

Estornell J, Ruiz LA, Velázquez-Martí B, Hermosilla T, 2012. Estimation of biomass and volumen of shrub vegetation using LiDAR and spectral data in a Mediterranean environment. Biomass Bioenerg 46: 710-721. https://doi.org/10.1016/j.biombioe.2012.06.023

EC (European Comission), 2017. https://ec.europa.eu/food/plant/plant_health_biosecurity/legislation/emergency_measures_en

Fassnacht FE, Latifi H, Stereńczak K, Modzelewska A, Lefsky M, Waser LT, Straub C, Ghosh A, 2016. Review of studies on tree species classification from remotely sensed data. Remote Sens Environ 186: 64-87. https://doi.org/10.1016/j.rse.2016.08.013

Fauzi A, Skidmore AK, Gils H, Schlerf M, Heitkönig I, 2013. Shrimp pond effluent dominates foliar nitrogen in disturbed mangroves as mapped using hyperspectral imagery. Marine Poll Bull 76: 42-51. https://doi.org/10.1016/j.marpolbul.2013.09.033

Fernández-García V, Santamarta M, Fernández-Manso A, Quintano C, Marcos E, Calvo L, 2018. Burn severity metrics in fire-prone pine ecosystems along a climatic gradient using Landsat imagery, Remote Sens Environ 206: 205-217. https://doi.org/10.1016/j.rse.2017.12.029

Fernández-Guisuraga JM, Sanz-Ablanedo E, Suárez-Seoane S, Calvo L, 2018. Using Unmanned Aerial Vehicles in Postfire Vegetation Survey Campaigns through Large and Heterogeneous Areas: Opportunities and Challenges. Sensors 18: 586. https://doi.org/10.3390/s18020586

Fernández-Landa A, Tomé JL, Sandoval VJ, Vallejo R, 2017. Integrando datos LiDAR, información satelital y parcelas del Inventario Forestal Nacional Español en la predicción de variables de inventario. 7º Congreso Forestal Español. 26-30 de junio de 2017. Plasencia, Cáceres, España.

Fernández-Landa A, Fernández-Moya J, Tomé JL, Algeet-Abarquero N, Guillén-Climent ML, Vallejo R, Sandoval V, Marchamalo M, 2018. High resolution forest inventory of pure and mixed stands at regional level combining National Forest Inventory field plots, Landsat, and low density LiDAR. Int J RemoteSens 39 (14):4830-4844. https://doi.org/10.1080/01431161.2018.1430406

Fernández-Manso O, Fernández-Manso A, Quintano C, 2014. Estimation of aboveground biomass in Mediterranean forests by statistical modelling of ASTER fraction images. Int J of Appl Earth Obs 31: 45-56. https://doi.org/10.1016/j.jag.2014.03.005

Fernández-Manso A, Quintano C, Roberts DA, 2016a. Burn severity influence on post-fire vegetation cover resilience from Landsat MESMA fraction images time series in Mediterranean forest ecosystems. Remote Sens Environ 184: 112-123. https://doi.org/10.1016/j.rse.2016.06.015

Fernández-Manso A, Fernández-Manso O, Quintano C, 2016b. SENTINEL-2A red-edge spectral indices suitability for discriminating burn severity. Int J of Appl Earth Obs 50: 170-175. https://doi.org/10.1016/j.jag.2016.03.005

García M, Riaño D, Chuvieco E, Danson FM, 2010. Estimating biomass carbon stocks for a Mediterranean forest in central Spain using LiDAR height and intensity data. RemoteSens. Environ. 114: 816–830. https://doi.org/10.1016/j.rse.2009.11.021

García M, Riaño D, Chuvieco E, Salas J, Danson FM, 2011. Multispectral and LiDAR data fusión for fuel type mapping using Support Vector Machine and decision rules. Remote Sens Environ 115: 1369-1379. https://doi.org/10.1016/j.rse.2011.01.017

García M, Popescu S, Riaño D, Zhao K, Neuenschwander A, Agca M, Chuvieco E, 2012. Characterization of canopy fuels using ICESat/GLAS data, Remote Sens Environ 123: 81-89. https://doi.org/10.1016/j.rse.2012.03.018

García-Álvarez D, Camacho Olmedo MT, 2017. Changes in the methodology used in the production of the Spanish CORINE: uncertainty analysis of the new maps. Int J of ApplEarthObs 63: 55-67. https://doi.org/10.1016/j.jag.2017.07.001

García-Gutiérrez J, González-Ferreiro E, Riquelme-Santos JC, Miranda D, Diéguez-Aranda U, Navarro-Cerrillo RM, 2014. Evolutionary feature selection to estimate forest stand variables using LiDAR, Int J of Appl Earth Obs 26: 119-131. https://doi.org/10.1016/j.jag.2013.06.005

Garestier F, Dubois-Fernández PC, Papathanassiou KP, 2008. Pine Forest Height Inversion Using Single-Pass X-Band PolInSAR Data. IEEE TransGeosci Rem Sens 46: 59-68. https://doi.org/10.1109/TGRS.2007.907602

Gastón A, Ciudad C, Mateo-Sánchez MC, García-Viñas JI, López-Leiva C, Fernández-Landa A, Marchamalo M,

Cuevas J, de la Fuente B, Fortin M-J, Saura S, 2017. Species' habitat use inferred from environmental variables at multiple scales: How much we gain from high-resolution vegetation data?Int J of Appl Earth Obs 55: 1-8. https://doi.org/10.1016/j.jag.2016.10.007

Gómez C, Wulder MA, Montes F, Delgado JA, 2011. Forest structural diversity characterization in Mediterranean pines of Central Spain with QuickBird-2 imagery and canonical correlation analysis. Can J Remote Sens 37 (6): 628-642. https://doi.org/10.5589/m12-005

Gómez C, Wulder MA, White JC, Montes F, Delgado JA, 2012a. Characterizing 25 years of change in the area, distribution, and carbon stock of Mediterranean pines in Central Spain. Int J Remote Sens 33 (17): 5546-5573. https://doi.org/10.1080/01431161.2012.663115

Gómez C, Wulder JA, Montes F, Delgado JA, 2012b. Modeling Forest Structural Parameters in the Mediterranean Pines of Central Spain using QuickBird-2 Imagery and Classification and Regression Tree Analysis (CART). Remote Sens-Basel 4 (1): 135-159. https://doi.org/10.3390/rs4010135

Gómez C, White JC, Wulder MA, Alejandro P, 2014. Historical forest biomass dynamics modelled with Landsat spectral trajectories. ISPRS J Photogramm93: 14-28.

Gómez C, Aulló-Maestro I, Montes F, 2016a. Dominant tree species dynamics informed by 30 years of Landsat time series in mountain areas of Northern Spain. ForestSAT 2016, Santiago (Chile), November, 15-18.

Gómez C, White JC, Wulder MA, 2016b. Optical remotely sensed time series data for land cover classification: A review. ISPRS Int J Remote Sens 116: 55-72. https://doi.org/10.1016/j.isprsjprs.2016.03.008

Gómez C, Green D, 2017. Small unmanned airborne systems to support oil and gas pipeline monitoring and mapping. Arab J Geosci 10 (9): 202. https://doi.org/10.1007/s12517-017-2989-x

Gómez C, Hermosilla T, Martínez-Fernández J, Montes F, Aulló-Maestro I, White JC, Wulder MA, Coops NC, Vázquez A, 2017. Annual cartography of fire (1985-2015) in forest areas of the NW Spain mapped with time series of Landsat data and Composite2Change. Nuevas plataformas y sensores de teledetección, XVII Congreso de la Asociación Española de Teledetección (Eds. Ruiz LA, Estornell J, Erena M), Murcia (Spain), October 3-7, pp: 169-172.

Gómez C, Aulló-Maestro I, Alejandro P, Montes F, 2018. Presence of European beech in its Spanish southernmost limit characterized with Landsat intra-annual time series. AIT2018 IX Conference of the Italian Society of Remote Sensing. Florence (Italy), July 4-6.

Gonçalves-Seco L, González-Ferreiro E, Diéguez-Aranda U, Fraga-Bugallo B, Crecente R, Miranda D, 2011. Assessomg the attributes of high-density Eucalyptus globulus stands using airborne laser scanner data. Int J RemoteSens 32(24): 9821-9841. https://doi.org/10.1080/01431161.2011.593583

González-Alonso F, Merino-de-Miguel S, Roldán-Zamarron A, García Gigorro S, Cuevas JM, 2006. Forest biomass estimation through NDVI composites. The role of remote sensed data to assess Spanish forests as carbon sinks. Int J RemoteSens, 27: 5409-5415. https://doi.org/10.01431160600830748

González-Ferreiro E, Diéguez-Aranda U, Miranda D, 2012. Estimation of stand variables in Pinusradiata D. Don plantations using different LiDAR pulse densities. Forestry 85: 281-292. https://doi.org/10.1093/forestry/cps002

González-Ferreiro E, Miranda D, Barreiro-Fernández L, Buján S, García-Gutiérrez J, Diéguez-Aranda U, 2013a. Modelling stand biomass fractions in Galician Eucalyptus globulus plantations by use of different LiDAR pulse densities. Forest Syst 22: 510-525. https://doi.org/10.5424/fs/2013223-03878

González-Ferreiro E, Diéguez-Aranda U, Barreiro-Fernández L, Buján S, Barbosa M, Suárez JC, Bye IJ, Miranda D, 2013b. A mixed pixel- and region-based approach for using airborne laser scanning data for individual tree crown delineation in Pinusradiata D. Don plantations. Int J RemoteSens 34(21): 7671-7690. https://doi.org/10.1080/01431161.2013.823523

González-Ferreiro E, Diéguez-Aranda U, Crecente-Campo F, Barreiro-Fernández L, Miranda D, Castedo-Dorado F, 2014. Modelling canopy fuel variables for Pinusradiata D. Don in NW Spain with low-density LiDAR data. I J Wild Fire 23(3): 350-362. https://doi.org/10.1071/WF13054

González-Ferreiro F, Arellano-Pérez S, Castedo-Dorado F, Hevia A, Vega JA, Vega-Nieva D, Álvarez-González JG, Ruiz-González AD, 2017. Modelling the vertical distribution of canopy fuel load using national forest inventory and low-density airborne laser scanning data. PLoS ONE 12(4): e0176114. https://doi.org/10.1371/journal.pone.0176114

González-Olabarría JR, Rodríguez F, Fernández-Landa A, Mola-Yudego B, 2012. Mapping fire risk in the model forest of Urbión (Spain) based on airborne LiDAR measurements. ForEcolManag 282: 149-156.

Gonzalo J, López D, Domínguez D, García A, Escapa A, 2017. On the capabilities and limitations of high altitude pseudo-satellites. Prog Aero Sci 98: 34-56.

Guerra-Hernández J, Görgens EB, García-Gutiérrez J, Carlos L, Rodríguez E, Tomé M, González-Ferreiro E, 2016. Comparison of ALS based models for estimating aboveground biomass in three types of Mediterranean forest. Eur. J. RemoteSens 49: 185–204. https://doi.org/10.5721/EuJRS20164911

Guerra-Hernández J, González-Ferreiro E, Monleón VJ, Faias SP, Tomé M, Díaz-Varela RA, 2017. Use of Multi-Temporal UAV-Derived Imagery for Estimating Individual Tree Growth in Pinuspinea Stands. Forests 8: 300. https://doi.org/10.3390/f8080300

Hall RJ, Castilla G, White JC, Cooke BJ, Skakun RS, 2016. Remote sensing of forest pest damage: a review and lessons learned from a Canadian perspective. Can Entomol 148: 1-61. https://doi.org/10.4039/tce.2016.11

Hajnsek I, Pottier E, Cloude SR, 2003. Inversion of Surface Parameters FromPolarimetric SAR. IEEE Trans Geosci Rem Sens 41: 727-744. https://doi.org/10.1109/TGRS.2003.810702

Henderson FM, Lewis AJ, 1998. Principles and applications of imaging radar. Manual of remote sensing: Third edition, Volume 2. United States. 896 pp.

Hermosilla T, Díaz-Manso JM, Ruiz LA, Recio JA, Fernández-Sarría A, Ferradáns-Nogueira P, 2012. Analysis of parcel-based image classification methods for monitoring the activities of the Land Bank of Galicia (Spain). ApplGeomat 4(4): 245-255. https://doi.org/10.1007/s12518-012-0087-z

Hermosilla T, Wulder MA, White JC, Coops NC, Hobart GW, 2015. An Integrated Landsat Time Series Protocol for Change Detection and Generation of Annual Gap-Free Surface Reflectance Composites. Remote Sens Environ 158: 220-234. https://doi.org/10.1016/j.rse.2014.11.005

Hermosilla T, Wulder MA, White JC, Coops NC, Hobart GW, Campbell LB, 2016. Mass data processing of time series Landsat imagery: pixels to data products for forest monitoring. Int J Digit Earth 9 (11): 1035-1054. https://doi.org/10.1080/17538947.2016.1187673

Hermosilla T, Wulder MA, White JC, Coops NC, Hobart GW, 2017. Updating Landsat time series of surface-reflectance composites and forest change products with new observations. Int J Appl Earth Obs 63: 104-111. https://doi.org/10.1016/j.jag.2017.07.013

Hermosilla T, Wulder MA, White JC, Coops NC, Hobart GW, 2018. Disturbance-informed annual land cover classification maps of Canada's forested ecosystems for a 29-year Landsat time series. Can J RemoteSens 44 (1): 67-87. https://doi.org/10.1080/07038992.2018.1437719

Hernández L, Martínez-Fernández J, Cañellas I, Vázquez de la Cueva A, 2014. Assessing spatio-temporal rates, patterns and determinants of biological invasions in forest ecosystems. The case of Acacia species in NW Spain, Forest EcolManag 329: 206-213. https://doi.org/10.1016/j.foreco.2014.05.058

Hernández-Clemente R, North PRJ, Hornero A, Zarco-Tejada PJ, 2017. Assessing the effects of forest health on sun-induced chlorophyll fluorescence using the FluorFLIGHT 3-D radiative transfer model to account for forest structure. Remote Sens Environ 193: 165-179. https://doi.org/10.1016/j.rse.2017.02.012

Hernando A, Velázquez J, Valbuena R, Legrand M, García-Abril A, 2017. Influence of the Resolution of Forest Cover Maps in Evaluating Fragmentation and Connectivity to Assess Habitat Conservation Status. EcolIndic 79: 295-302. https://doi.org/10.1016/j.ecolind.2017.04.031

Hernando A, Puerto L, Mola-Yudego B, Manzanera J, García-Abril A, Maltamo M, Valbuena R, 2019. Estimation of forestbiomasscomponentsthroughairborneLiDAR and multispectralsensors. iForest

Hevia A, Álvarez-González JG, Ruiz Fernández E, Prendes C, Ruiz González AD, Majada J, González-Ferreiro E, 2016. Modelling canopy fuel and forest stand variables and characterizing the influence of thinning in the stand structure using airborne LiDAR. Revista Teledetección 45: 41-55. https://doi.org/10.4995/raet.2016.3979

Hilker T, Wulder MA, Coops NC, 2008. Update of forest inventory data with LiDAR and high spatial resolution satellite imagery. Can J Remote Sens 34: 5-12. https://doi.org/10.5589/m08-004

Huang H, Roy DO, Boschetti L, Zhang HK, Yan L, Kumar SS, Gómez-Dans J, Li J, 2016. Separability analysis of Sentinel-2A multi-spectral instrument (MSI) data for burned area discrimination. RemoteSens-Basel 8: 973. https://doi.org/10.3390/rs8100873

Huesca M, Merino-de-Miguel S, González-Alonso F, 2013a. An intercomparison of satellite burned area maps derived from MODIS, MERIS, SPOT-VEGETATION and ATSR images. An application to the August 2006 Galicia (Spain) forest fires. For Syst 22 (2): 222-231.

Huesca M, Merino-de-Miguel S, González-Alonso F, Martínez S, Cuevas JM, Calle A, 2013b. Using AHS hyper-spectral images to study forest vegetation recovery after a fire. Int J Remote Sens 34 (11): 4025-4048. https://doi.org/10.1080/01431161.2013.772313

Hyyppä J, Inkinen M, 1999. Detecting and estimating attributes for single tree using laser scanner. Phot J Fin 16: 27-42.

INE 2017. España en cifras. https://www.ine.es/prodyser/espa_cifras/2017/index.html#5

Jensen J, 2005. Introductory digital image processing: a remote sensing perspective, 3rd ed. Pearson Education, Inc. 526 pp.

Joshi N, Mitchard ETA, Brolly M, Schumacher J, Fernández-Landa A, Johannsen VK, Marchamalo M, Fensholt R, 2017. Understanding 'saturation' of radar signals over forests. Sci Rep-UK 7 (1): 3505. https://doi.org/10.1038/s41598-017-03469-3

Karnkowski W, Sahajdak A, 2010. Occurrence of the pinewood nematode in Portugal and Spain - Threat for pine forests in Europe. Prog Plant Prot 50: 1260-1264.

Keane RE, Burgan R, Wagtendonk JV, 2001. Mapping wildland fuels for fire management across multiple scales: Integrating remote sensing, GIS, and biophysical modeling, Int J Wildand Fire 10: 301-319. https://doi.org/10.1071/WF01028

Kennedy RE, Yang Z, Cohen WB, 2010. Detecting trends in forest disturbance and recovery using yearly Landsat time series: 1. LandTrendr-temporal segmentation algorithms. Remote Sens Environ 114: 2897-2910. https://doi.org/10.1016/j.rse.2010.07.008

Kennedy RE, Yang Z, Braaten J, Copass C, Antonova N, Jordan C, Nelson P, 2015. Attribution of disturbance change agent from Landsat time-series in support of habitat monitoring in the Puget Sound region, USA. Remote Sens Environ 166: 271-285. https://doi.org/10.1016/j.rse.2015.05.005

Key CH, Benson NC, 1999. Measuring and remote sensing of burn severity. In L. F. Neuenschwander and K. C. Ryan (Eds.), Proceedings Joint Fire Science Conference and Workshop, Vol. II. (pp. 284). Moscow, ID: University of Idaho and International Association of Wildland Fire.

Kissinger G, Herold M, De Sy V, 2012. Drivers of Deforestation and Forest Degradation: A Synthesis Report for REDD+ Policymakers. Lexeme Consulting, Vancouver Canada, 46 pp.

Le Toan T, Beaudoin A, Guyon D, 1992. Relating forest biomass to SAR data. IEEE Trans Geosci Rem Sens 30: 403-411. https://doi.org/10.1109/36.134089

Le Toan T, Quegan S, Davidson MWJ, Balzter H, Paillou P, Papathanassiou K, Plummer S, Rocca F, Saatchi S, Shugart H, Ulander LMH, 2011. The BIOMASS mission: Mapping global forest biomass to better understand the terrestrial carbon cycle. Remote Sens Environ 115: 2850-2860. https://doi.org/10.1016/j.rse.2011.03.020

Leberl F, Irschara A, Pock T, Meixner P, Gruber M, Scholz S, Wiechert A, 2010. Point clouds: LiDAR versus three dimensional vision. PhotogrammEng Rem Sens76: 1123-1134.

Lefsky MA, Cohen WB, Acker SA, Parker GG, Spies TA, Harding D, 1999. LiDAR remote sensing of the canopy structure and biophysical properties of Douglas-fir western hemlock forests. Remote Sens Environ 70: 339-361. https://doi.org/10.1016/S0034-4257(99)00052-8

Lefsky MA, 2010. A global forest canopy height map from the Moderate Resolution Imaging Spectroradiometer and the Geoscience Laser Altimeter System. Geophys Res Lett 37 L15401. https://doi.org/10.1029/2010GL043622

Li J, Roy DP, 2017. A global analysis of Sentinel-2A, Sentinel-2B and Landsat-8 data revisit intervals and implications for terrestrial monitoring. Remote Sens-Basel 9: 902. https://doi.org/10.3390/rs9090902

Lisein J, Pierrot-Deseilligny M, Bonnet, S, Lejeune P, 2013. A Photogrammetric Workflow for the Creation of a Forest Canopy Height Model from Small Unmanned Aerial System Imagery. Forests 4: 922-944. https://doi.org/10.3390/f4040922

Lohberger S, Stängel M, Atwood EC, Siegert F, 2018. Spatial evaluation of Indonesia's 2015 fire-affected area and estimated carbon emissions using Sentinel-1. Glob Chang Biol 24 (2): 644-654. https://doi.org/10.1111/gcb.13841

López-Sánchez JM, Ballester-Berman JD, 2009. Potentials of Polarimetric SAR Interferometry for Agriculture Monitoring. Radio Sci 44: RS2010. https://doi.org/10.1029/2008RS004078

Malak DA, Pausas JG, Pardo-Pascual JE, Ruiz LA, 2015. Fire recurrence and the dynamics of the Enhanced Vegetation Index in a Mediterranean ecosystem. Int J App Geosp Res 6 (2): 18-35. https://doi.org/10.4018/ijagr.2015040102

Manfreda S, McCabe MF, Miller PE, Lucas R, Pajuelo Madrigal V, Mallinis G, Ben Dor E, Helman D, Estes L, Ciraolo G, *et al.*, 2018. On the Use of Unmanned Aerial Systems for Environmental Monitoring. RemoteSens-Basel 10: 641. https://doi.org/10.3390/rs10040641

Manzanera JA, García-Abril A, Pascual C, Tejera R, Martín-Fernández S, Tokola T, Valbuena R, 2016. Fusion of airborne LiDAR and multispectral sensors reveals synergic capabilities in forest structure characterization. GISci Rem Sens 53(6): 723-738. https://doi.org/10.1080/15481603.2016.1231605

MAPAMA, 2011. Anuario de estadística forestal. Ministerio de Agricultura, Alimentación y Medio Ambiente, Spain, 103 pp

Marino E, Ranz P, Tomé JL, Noriega MA, Esteban J, Madrigal J, 2016. Generation of high-resolution fuel models from discrete airborne laser scanner and Landsat-8 OLI: a low-cost and highly updated methodology for large areas. Remote Sens Environ 187: 267-280. https://doi.org/10.1016/j.rse.2016.10.020

Marino E, Tomé JL, Madrigal J, Guijarro M, Hernando C, 2017a. Efecto de la densidad de pulsos LiDAR en la caracterización estructural de combustibles en masas de pinar. 7º Congreso Forestal Español. 26-30 de junio de 2017. Plasencia, Cáceres, España.

Marino E, Ranz P, Tomé JL, 2017b. Evolución post-incendio de la estructura de la vegetación en el PN de Garajonay a partir de datos LiDAR. 7º Congreso Forestal Español. 26-30 de junio de 2017. Plasencia, Cáceres, España.

Marino E, Montes F, Tomé JL, Navarro JA, Hernando C, 2018. Vertical forest structure analysis for wildfire prevention: comparing airborne laser scanning data and stereoscopic hemispherical images. Int J Appl Earth 73: 438-449. https://doi.org/10.1016/j.jag.2018.07.015

Martín-Alcón S, CollLl, de Cáceres M, Guitart L, Cabré M, Just A, González-Olabarría JR, 2015. Combining aerial LiDAR and multi-spectral imagery to assess post-fire regeneration types in a Mediterranean forest. Can J For Res 45 (7): 856-866. https://doi.org/10.1139/cjfr-2014-0430

Martínez S, Chuvieco E, Aguado I, Salas J, 2017. Severidad y regeneración en grandes incendios forestales: análisis a partir de series temporales de imágenes Landsat. Revista de Teledetección 49: 17-32. https://doi.org/10.4995/raet.2017.7182

Martínez-Fernández J, Ruiz-Benito P, Bonet-Jornet A, Gómez C, 2019. Methodological variations in the production of CORINE Land Cover and consequences for long-term land cover change studies. The case of Spain. Int J Remote Sens.

Matasci G, Hermosilla T, Wulder MA, White JC, Coops NC, Hobart GW, Zald HSJ, 2018. Large-area mapping of Canadian boreal forest cover, height, biomass and other structural attributes using Landsat composites and LiDAR plots. Remote Sens Environ 209: 90-106. https://doi.org/10.1016/j.rse.2017.12.020

Mauro F, Valbuena R, Manzanera JA, García-Abril A, 2011. Influence of Global Navigation Satellite System errors in positioning inventory plots for tree-height distribution studies. Can J For Res 41 (1): 11-23. https://doi.org/10.1139/X10-164

Mauro F, Molina I, García-Abril A, Valbuena R, Ayuga-Téllez E, 2016. Remote sensing estimates and measures of uncertainty for forest variables at different aggregation levels. Environmetrics 27 (4): 225-238. https://doi.org/10.1002/env.2387

Mauro F, Monleón VJ, Temesgen H, Ford KR, 2017a. Analysis of area level and unit level models for small area estimation in forest inventories assisted with LiDAR auxiliary information. PloS ONE 12 (12), e0189401 https://doi.org/10.1371/journal.pone.0189401

Mauro F, Monleón VJ, Temesgen H, Ruiz LA, 2017b. Analysis of spatial correlation in predictive models of forest variables that use LiDAR auxiliary information. Can J For Res 47 (6): 788-799. https://doi.org/10.1139/cjfr-2016-0296

Melicharová L, Vizoso-Arribe O, 2012. Situation of sweet chestnut (Castaneasativa Mill.) in Spain, Galicia: A review. ScientiaAgrBoh 2012: 78-84.

Méndez E, Valés JJ, Pino I, Granado L, Montoya G, Prieto R, Carpintero IR, Giménez de Azcárate F, Cáceres F, Moreira JM, *et al.*, 2016. Determination of forest biomass using remote sensing techniques with radar images. Pilot study in area of the province of Huelva. REDIAM. Revista de Teledetección 45: 71-86. https://doi.org/10.4995/raet.2016.3984

Merino de Miguel S, Huesca M, González-Alonso F, 2010. MODIS reflectance and active fire data for burn mapping and assessment at regional level. Ecol Model 221: 67-74. https://doi.org/10.1016/j.ecolmodel.2009.09.015

Moessner KE, 1953. Photo interpretation in forest inventories. PhotogrammEng, June 1953: 496-507.

Montealegre AL, Lamelas MT, de la Riva J, García-Martín A, Escribano F, 2016. Use of low point density ALS data to estimate stand-level structural variables in Mediterranean Aleppo pine forest. Forestry 0: 1-10. https://doi.org/10.1093/forestry/cpw008

Montealegre AL, Lamelas MT, Tanase MA, de la Riva J, 2017a. Estimación de la severidad en incendios forestales a partir de datos LiDAR-PNOA y valores de CompositeBurnIndex. Revista de Teledetección 49: 1-16. https://doi.org/10.4995/raet.2017.7371

Montealegre AL, Lamelas-Gracia MT, García-Martín A, de la Riva-Fernández J, Escribano-Bernal F, 2017b. Using low density discrete Airborne Laser Scanning data to assess the potential carbon dioxide emission in case of a fire event in a Mediterranean pine forest. GISci Rem Sens 54 (5): 721-740. https://doi.org/10.1080/15481603.2017.1320863

Montero G, Ruiz-Peinado R, Muñoz M, 2005. Producción de biomasa y fijación de CO2 por los bosques españoles. Monografías Instituto Nacional de Investigación y Tecnología Agraria y Alimentaria, Serie Forestal, Madrid, Spain.

Montero G, Serrada R, 2013. La situación de los bosques y el sector forestal en España-ISFE 2013. Sociedad Española de Ciencias Forestales. Lourizán (Pontevedra), Spain. 257 pp.

Moreira A, Krieger G, Hajnsek I, Papathanassiou K, Younis M, Lopez-Dekker P, Huber S, Villano M, Pardini M, Eineder M, *et al.*, 2015. Tandem-L/ALOSNext: A Highly Innovative Bistatic SAR Mission for Global Observation of Dynamic Processes on the Earth's Surface. IEEE Geosc Remote Sens Mag 3 (2): 8-23. https://doi.org/10.1109/MGRS.2015.2437353

Næsset E, 2002. Predicting forest stand characteristics with airborne scanning laser using a practical two-stage procedure and field data. Remote Sens Environ 80: 88-99. https://doi.org/10.1016/S0034-4257(01)00290-5

Navarro JA, Fernández-Landa A, Tomé JL, Guillén-Climent ML, Ojeda JC, 2018. Testing the quality of forest variable estimation using dense image matching: a comparison with airborne laser scanning in a Mediterranean pine forest. Int J Rem Sens 39 (14): 4744-4760. https://doi.org/10.1080/01431161.2018.1471551

Navarro-Cerrillo RM, González-Ferreiro E, García-Gutiérrez J, Ceacero Ruiz CJ, Hernández-Clemente R, 2017. Impact of plot size and model selection on forest biomass estimation using airborne LiDAR: A case study of pine plantations in southern Spain. J For Sci 63: 88-97. https://doi.org/10.17221/86/2016-JFS

Oeser J, Pflugmacher D, Senf C, Heurich M, Hostert P, 2017. Using intra-annual Landsat time series for attributing forest disturbance agents in Central Europe. Forests 8: 251. https://doi.org/10.3390/f8070251

Olesk A, Praks J, Antropov O, Zalite K, Arumäe T, Voormansik K, 2016. Interferometric SAR coherence models for characterization of hemiboreal forests using TanDEM-X data. Remote Sens-Basel 8: 700. https://doi.org/10.3390/rs8090700

Packalén P, Maltamo M, 2006. Predicting the plot volume by tree species using airborne laser scanning and aerial photographs. Forest Sci 52: 611−622.

Packalén P, Suvanto A, Maltamo M, 2009. A two stage method to estimate species-specific growing stock. PhotogrammEng Rem Sens 75: 1451−1460. https://doi.org/10.14358/PERS.75.12.1451

Pajares G, 2015. Overview and current status of remote sensing applications based on Unmanned Aerial

Vehicles (UAVs). PhotogrammEng Rem Sens 81 (4): 281-329. https://doi.org/10.14358/PERS.81.4.281

Parra A, Chuvieco E, 2005. Assessing burn severity using Hyperion data. In J Riva, Pérez-Cabello F, Chuvieco E (Eds.) Proceedings of the 5th international workshop on remote sensing and GIS applications to forest fire management: fire effects assessment (pp 239-244) Paris. Universidad d Zaragoza, GOFC-GOLD, EARSeL.

Pascual A, Pukkala T, Rodríguez F, de-Miguel S, 2016. Using Spatial Optimization to Create Dynamic Harvest Blocks from LiDAR-Based Small Interpretation Units. Forests 7(10): 220. https://doi.org/10.3390/f7100220

Pascual A, Pukkala T, de-Miguel S, 2018a. Effects of plot positioning errors on the optimality of harvest prescriptions in spatial forest planning based on ALS data. Forests 9(7): 371. https://doi.org/10.3390/f9070371

Pascual A, Pukkala T, de-Miguel S, Pesonen A, Packalen P, 2018b. Influence of timber harvesting costs on the layout of cuttings and economic return in forest planning based on dynamic treatment units. ForSyst 27:1.

Pascual C, García-Abril A, García-Montero LG, Martín-Fernández S, Cohen WB, 2008. Object-based semi-automatic approach for forest structure characterization using LIDAR data in heterogeneous Pinussylvestris stands. Forest EcolManag 255: 3677-3685. https://doi.org/10.1016/j.foreco.2008.02.055

Pascual C, García-Abril A, Cohen WB, Martín-Fernández S, 2010. Relationship between LiDAR-derived forest canopy height and Landsat images. Int J RemoteSens 31 (5): 1261-1280. https://doi.org/10.1080/01431160903380656

Pascual C, García-Montero LG, Arroyo LA, García-Abril A, 2013. Increasing the use of expert opinion in forest characterisation approaches based on LiDAR data. Annals of Forest Science 70: 87-99. https://doi.org/10.1007/s13595-012-0232-1

Pasquarella VJ, Holden CE, Kaufman L, Woodcock CE, 2016. From imagery to ecology: leveraging time series of all available Landsat observations to map and monitor ecosystem state and dynamics. Rem Sens EcolConserv 2 (3): 151-170. https://doi.org/10.1002/rse2.24

Pasquarella VJ, Bradley BA, Woodcock CE, 2017. Near-Real-Time Monitoring of Insect Defoliation Using Landsat Time Series. Forests 8 (8): 275. https://doi.org/10.3390/f8080275

Pulliainen JT, Heiska K, Hyyappa J, Hallikainen MT, 1994. Backscattering properties of boreal forests at the C- and X-Bands. IEEE Trans Geosci Rem Sens, 32, 1041-1050. https://doi.org/10.1109/36.312892

Qi W, Dubayah RO, 2016. Combining Tandem-X InSAR and simulated GEDI LiDAR observations for forest structure mapping. Remote Sens Environ 187: 253-266. https://doi.org/10.1016/j.rse.2016.10.018

Quintano C, Fernández-Manso A, Fernández-Manos O, Shimabukuro YE, 2006. Mapping burned areas in Mediterranean countries using spectral mixture analysis from a uni-temporal perspective. Int J RemoteSens 27(4): 645-662. https://doi.org/10.1080/01431160500212195

Quintano C, Fernández-Manso A, Calvo L, Marcos E, Valbuena L, 2015. Land Surface temperature as potential indicator of burn severity in forest Mediterranean ecosystems. Int J ApplEarth 36: 1-12. https://doi.org/10.1016/j.jag.2014.10.015

Quintano C, Fernández-Manso A, Fernández-Manso O, 2018. Combination of Landsat and Sentinel-2 MSI data for initial assessing of burn severity. Int J Appl Earth ObsGeoinformation 64: 221-225. https://doi.org/10.1016/j.jag.2017.09.014

Radeloff VC, Mildenoff DJ, Boyce MS, 1999. Detecting Jack Pine budworm defoliation using spectral mixture analysis: separating effects from determinants. Remote Sens Environ 69: 156-169. https://doi.org/10.1016/S0034-4257(99)00008-5

Regos A, Ninyerola M, Moré G, Pons X, 2015. Linking land cover dynamics with driving forces in mountain landscape of the Northwestern Iberian Peninsula. Int J ApplEarth 38: 1-14. https://doi.org/10.1016/j.jag.2014.11.010

Riaño D, Chuvieco E, Salas J, Palacios-Orueta A, Bastarrika A, 2002. Generation of fuel type maps from Landsat TM images and ancillary data in Mediterranean ecosystems. Can J Forest Res 32: 1301-1315. https://doi.org/10.1139/x02-052

Riaño D, Chuvieco E, Condés S, González-Matesanz J, Ustin SL, 2004. Generation of crown bulk density for Pinussylvestris L. from LiDAR. Remote Sens Environ 92: 345-352. https://doi.org/10.1016/j.rse.2003.12.014

Rignot EJ, Way J, Williams C, Viereck L, 1994. Radar Estimates of Aboveground Biomass in Boreal Forests of Interior Alaska. IEEE TransGeosci Rem Sens 32: 1117-1124. https://doi.org/10.1109/36.312903

Robles A, Rodríguez-Garrido MA, Álvarez-Taboada MF, 2016. Characterization of wildland-urban interfaces using LiDAR data to estimate the risk of wildfire damage. Revista de Teledetección. (Special Issue): 57-69.

Rock BN, Vogelmann JE, Williams DL, Vogehnann AF, Hoshizaki T, 1986. Remote detection of forest damage. Bioscience 36: 439–445. https://doi.org/10.2307/1310339

Rubio A, Gavilán RG, Montes F, Gutiérrez-Girón A, Díaz-Pines E, Mezquida ET, 2011. Biodiversity measures applied to stand-level management: Can they really be useful? EcolIndic 11: 545-556. https://doi.org/10.1016/j.ecolind.2010.07.011

Ruiz LA, Recio JA, Fenández-Sarría A, 2005. Clasificación de entornos forestales mediterráneos mediante técnicas de análisis de texturas. Cuadernos de la Sociedad Española de Ciencias Forestales (SECF) 19: 187-192.

Ruiz LA, Hermosilla T, Mauro F, Godino M, 2014. Analysis of the influence of plot size and LiDAR density on forest structure attribute estimates. Forests 5 (5): 936-957. https://doi.org/10.3390/f5050936

Ruiz LA, Recio JA, Crespo-Peremarch P, Sapena M, 2018. An object-based approach for mapping forest structural types based on low density LiDAR and multispectral imagery. GeocartoInt 33: 443-457. https://doi.org/10.1080/10106049.2016.1265595

Ruiz-Gallardo JR, Castaño S, Calera A, 2004. Application of remote sensing and GIS to locate priority intervention areas after wildland fires in Mediterranean systems: a case study from south-eastern Spain. Int J Wildland Fire 13: 241-252. https://doi.org/10.1071/WF02057

Ruiz-Peinado R, Del Rio M, Montero G, 2011. New models for estimating the carbon sink capacity of Spanish softwood species. For Syst 20: 176-188.

Rullán-Silva CD, Olthoff AE, Delgado JA, Pajares-Alonso JA, 2013. Remote monitoring of forest insect defoliation. A review. Forest Syst 22 (3): 377-391. https://doi.org/10.5424/fs/2013223-04417

Rullán-Silva C, Olthoff AE, Pando V, Pajares JA, Delgado JA, 2015. Remote monitoring of defoliation by the beech leaf-mining weevil Rhynchaenusfagi in northern Spain. Forest EcolManag 347: 200-208. https://doi.org/10.1016/j.foreco.2015.03.005

Sandberg G, Ulander LMH, Fransson JES, Holmgren J, Toan TL, 2011. L- and P-band backscatter intensity for biomass retrieval in hemiboreal forest. Remote Sens Environ 115: 2874-2886. https://doi.org/10.1016/j.rse.2010.03.018

Sangüesa-Barreda G, Camarero JJ, García-Martín A, Rodolfo Hernández R, de la Riva J, 2014. Remote-sensing and tree-ring based characterization of forest defoliation and growth loss due to the Mediterranean pine processionary moth. Forest EcolManag 320: 171-181. https://doi.org/10.1016/j.foreco.2014.03.008

Sangüesa-Barreda G, Camarero JJ, Oliva J, Montes F, Gazol A, 2015. Past logging, drought and pathogens interact and contribute to forest dieback. Agric For Meteorol 208: 85-94. https://doi.org/10.1016/j.agrformet.2015.04.011

Sankey T, Donager J, McVay J, Sankey JB, 2017. UAV LiDAR and hyperspectral fusion for forest monitoring in the southwestern USA. Remote Sens Environ 195: 30-43. https://doi.org/10.1016/j.rse.2017.04.007

Schlerf M, Atzberger C, Hill J, Buddenbaum H, Werner W, Schuler G, 2010. Retrieval of chlorophyll and nitrogen in Norway spruce (Piceaabies L. Karst.) using imaging spectroscopy. Int J Appl Earth 12: 17-26. https://doi.org/10.1016/j.jag.2009.08.006

Schutz BE, Zwally HJ, Shuman CA, Hancock D, DiMarzio JP, 2005. Overview of the ICESat Mission, Geophys Res Lett 32: L21S01. https://doi.org/10.1029/2005GL024009

Sevillano-Marco E, Fernández-Manso A, Quintano C, Poulain M, 2013. CCD CBERS and ASTER data in dasometric characterization of Pinusradiata D. Don (North-Western Spain). Cerne, Lavras 19(1): 103-110.

Shimada M, Itoh T, Motooka T, Watanabe M, Shiraishi T, Thapa R, Lucas R, 2014. New global forest/non-forest maps from ALOS PALSAR data (2007–2010). Remote Sens Environ 155: 13-31. https://doi.org/10.1016/j.rse.2014.04.014

Sherald J, 2007. Bacterial Leaf Scorch of Landscape Trees: What We Know and What We Do Not Know. Arb Urb Forestry 33.

Simonson W, Allen H, Coomes D, 2018. Effect of Tree Phenology on LiDAR Measurement of Mediterranean Forest Structure. RemoteSens 10: 659 https://doi.org/10.3390/rs10050659

Silveira EM, de Mello JM, Acerbi FW, dos Reis AA, Withey KD, Ruiz LA, 2018. Characterizing landscape spatial heterogeneity using semivariogram parameters derived from NDVI images. CERNE, 23 (4): 413-422. https://doi.org/10.1590/01047760201723042370

Smith MW, Carrivick J, Quincey D, 2016. Structure from Motion Photogrammetry in Physical Geography. Prog Phys Geog 40 (2): 247-275. https://doi.org/10.1177/0309133315615805

Tanase M, Santoro M, Wegmüller U, de la Riva J, Pérez-Cabello F, 2010b. Properties of X-, C- and L-band repeat-pass interferometric SAR coherence in Mediterranean pine forests affected by fires, Remote Sens Environ 114: 2182-2194. https://doi.org/10.1016/j.rse.2010.04.021

Tanase MA, de la Riva J, Pérez-Cabello F, 2011a. Estimating burn severity at the regional level using optically based indices. Can J For Res 41: 863-872. https://doi.org/10.1139/x11-011

Tanase MA, de la Riva J, Santoro M, Pérez-Cabello F, Kasischke E, 2011b. Sensitivity of SAR data to post-fire forest regrowth in Mediterranean and boreal forests. Remote Sens Environ 115: 2075-2085. https://doi.org/10.1016/j.rse.2011.04.009

Tanase MA, Panciera R, Lowell K, Tian S, García-Martín A, Walker JP, 2014a. Sensitivity of L-band radar backscatter to forest biomass in semi-arid environments: a comparative analysis of parametric and non-parametric models. IEEE Trans Geosci Rem Sens: 52, 1-15. https://doi.org/10.1109/TGRS.2013.2283521

Tanase MA, Panciera R, Lowell K, Aponte C, Hacker JM, Walker JP, 2014b. Forest biomass estimation at high spatial resolution: Radar vs. LiDAR sensors. IEEE TransGeosci Rem SensLett 11 (3): 711-715. https://doi.org/10.1109/LGRS.2013.2276947

Tanase MA, Santoro M, Aponte C, De la Riva J, 2014c. Polarimetric Properties of Burned Forest Areas at C- and L-Band. IEEE Trans Geosci Rem Sens 7 (1): 267-276.

Tanase MA, Kennedy R, Aponte C, 2015a. Fire severity from space: a comparison of active and passive sensors and their synergy for different forest types. Int J Wildland Fire 24(8): 1062-1075. https://doi.org/10.1071/WF15059

Tanase MA, Kennedy R, Aponte C, 2015b. Radar Burn Ratio for fire severity estimation at canopy level: an example for temperate forests. Remote Sens Environ 170: 14-31. https://doi.org/10.1016/j.rse.2015.08.025

Tanase MA, Panciera R, Lowell K, Aponte C, 2015c. Monitoring live fuel moisture in semi-arid environments using L-band radar data. Int J Wildland Fire 24: 560-572. https://doi.org/10.1071/WF14149

Tanase MA, Aponte C, Mermoz S, Bouvet A, Le Toan T, Heurich M, 2018. Detection of windthrows and insect outbreaks by L-band SAR: A case study in the Bavarian Forest National Park. Remote Sens Environ 209: 700-711. https://doi.org/10.1016/j.rse.2018.03.009

Tebaldini S, Rocca F, 2012. MultibaselinePolarimetric SAR Tomography of a Boreal Forest at P- and L-Bands. IEEE T GeosciRemote 50: 232-246. https://doi.org/10.1109/TGRS.2011.2159614

Tomé JL, Esteban J, Martín-Alcón S, Escamochero I, Fernández-Landa A, 2017. Forestmap, inventario forestal online a partir de datos LiDAR en la Región de Murcia. Nuevas plataformas y sensores de teledetección, XVII Congreso de la Asociación Española de Teledetección (Eds. Ruiz LA, Estornell J, Erena M), Murcia (Spain), October 3-7, pp: 147-150.

Tompalski P, Coops NC, Marshall PL, White JC, Wulder MA, Bailey T, 2018. Combining multi-date airborne laser scanning and digital aerial photogrammetric data for forest growth and yield modelling. Remote Sens-Basel 10: 347. https://doi.org/10.3390/rs10020347

Tomppo E, Olsson H, Stahl G, Nilsson M, Hagner O, Katila M, 2008. Combining national forest inventory field plots and remote sensing data for forest databases. Remote Sens Environ 112: 1982-1999. https://doi.org/10.1016/j.rse.2007.03.032

Torresan C, Beaton A, Carotenuto F, Filippo S, Gioli B, Matese A, Miglietta F, Magnoli C, Zaldea A, Wallace L, 2017. Forestry applications of UAVs in Europe: a review. Int J Remote Sens 38 (8-10): 2427-2447. https://doi.org/10.1080/01431161.2016.1252477

Transon J, Andrimont R, Maugnard A, Defourny P, 2018. Survey of hyperspectral Earth Observation applications from space in the Sentinel-2 context. RemoteSens-Basel 10: 157. https://doi.org/10.3390/rs10020157

Trassierra A, Esteban J, Fernández-Landa A, Sabín P, Sánchez-Pellicer T, Tomé JL, 2017. Modelos de estimación de carga de biomasa aérea de matorral a partir de diferentes fuentes de información: LiDAR y Landsat. 7º Congreso Forestal Español. 26-30 de junio de 2017. Plasencia, Cáceres, España.

Turner DP, Cohen WB, Kennedy RE, Fassnacht KS, Briggs JM, 1999. Relationship between leaf area index and Landsat TM spectral vegetation indices across three temperate zone sites. Remote Sens Environ 70: 52-68. https://doi.org/10.1016/S0034-4257(99)00057-7

UNECE (United Nations Economic Commission For Europe) ICP Forests Programme Co-ordinating Centre (Ed.), 2016, Manual on Methods and Criteria for Harmonized Sampling, Assessment, Monitoring and Analysis of the Effects of Air Pollution on Forests. Thunen Institute of Forest Ecosystems, Eberswalde. http://icp-forests.net/page/icp-forests-manual

Ungar S, Pearlman J, Mendenhall J, Reuter D, 2003. Overview of the Earth Observing-1 (EO-1) mission. IEEE T Geosci Remote 41: 1149−1159. https://doi.org/10.1109/TGRS.2003.815999

Valbuena R, Mauro F, Arjonilla FJ, Manzanera JA, 2011. Comparing Airborne Laser Scanning-Imagery Fusion Methods Based on Geometric Accuracy in Forested Areas. Remote Sens Environ 115(8): 1942-1956. https://doi.org/10.1016/j.rse.2011.03.017

Valbuena R, Mauro F, Rodríguez-Solano R, Manzanera JA, 2012. Partial Least Squares for Discriminating Variance Components in GNSS Accuracy Obtained Under Scots Pine Canopies. Forest Sci 58(2): 139-153. https://doi.org/10.5849/forsci.10-025

Valbuena R, De Blas A, Martín Fernández S, Maltamo M, Nabuurs GJ, Manzanera JA, 2013a. Within-Species Benefits of Back-projecting Laser Scanner and Multispectral Sensors in Monospecific P. sylvestris Forests. Eur J Remote Sens 46: 401-416. https://doi.org/10.5721/EuJRS20134629

Valbuena R, Maltamo M, Martín-Fernández S, Packalen P, Pascual C, Nabuurs G-J, 2013b. Patterns of covariance between airborne laser scanning metrics and Lorenz curve descriptors of tree size inequality. Can J RemoteSens 39(1): 18-31. https://doi.org/10.5589/m13-012

Valbuena R, Packalen P, García-Abril A, Mehtätalo L, Maltamo M, 2013c. Characterizing Forest Structural Types and Shelterwood Dynamics from Lorenz-based Indicators Predicted by Airborne Laser Scanning. Can J For Res 43: 1063-1074. https://doi.org/10.1139/cjfr-2013-0147

Valbuena R, Maltamo M, Packalen P, 2016a. Classification of Multi-Layered Forest Development Classes from Low-Density National Airborne LiDAR Datasets. Forestry 89: 392-341. https://doi.org/10.1093/forestry/cpw010

Valbuena R, Maltamo M, Packalen P, 2016b. Classification of Forest Development Stages from National Low-Density LiDAR Datasets: a Comparison of Machine Learning Methods. Revista de Teledetección 45: 15-25. https://doi.org/10.4995/raet.2016.4029

Valbuena R, Hernando A, Manzanera JA, Martínez-Falero E, García-Abril A, Mola-Yudego B, 2017a. Most Similar Neighbour Imputation of Forest Attributes Using Metrics Derived from Combined Airborne LIDAR and Multispectral Sensors. Int J DigitEarth 11 (12): 1205-1218. https://doi.org/10.1080/17538947.2017.1387183

Valbuena R, Hernando A, Manzanera JA, Görgens EB, Almeida DRA, Mauro F, García-Abril A, Coomes DA, 2017b. Enhancing of accuracy assessment for forest above-ground biomass estimates obtained from remote sensing via hypothesis testing and overfitting

evaluation. Eco Mod 622: 15-26. https://doi.org/10.1016/j.ecolmodel.2017.10.009

Valbuena-Rabadán M, Santamaría-Peña J, Sanz-Adán F, 2016. Estimation of diameter and height of individual trees for Pinussylvestris L. based on the individualising of crowns using airborne LiDAR and the National Forest Inventory data. ForSys 25(1): e046

Varo-Martínez MA, Navarro-Cerrillo RM, Hernández-Clemente R, Duque-Lazo J, 2017. Semi-automated stand delineation in Mediterranean Pinussylvestris plantations through segmentation of LiDAR data: The influence of pulse density. Int J ApplEarthObs 56: 54-64. https://doi.org/10.1016/j.jag.2016.12.002

Vázquez de la Cueva A, 2008. Structural attributes of three forest types in central Spain and Landsat ETM+ information evaluated with redundancy analysis. Int J Remote Sens 29: 5657-5676. https://doi.org/10.1080/01431160801891853

Verdú F, Salas J, 2010. Cartografía de áreas quemadas mediante análisis visual de imágenes de satélite en la España peninsular para el periodo 1991–2005. Geofocus 10: 54–81.

Viana-Soto A, Aguado I, Martínez S, 2017. Assessment of post-fire vegetation recovery using fire severity and geographical data in the Mediterranean region (Spain). Environments 4: 90. https://doi.org/10.3390/environments4040090

Vicente-Serrano SG, Pérez-Cabello F, Lasanta T, 2011. Pinushalepensis regeneration after a wildfire in a semiarid environment: assessment using multitemporal Landsat images. Int J Wildland Fire 20Ñ 195-208.

Viedma O, Quesada J, Torres I, De Santis A, Moreno JM, 2015. Fire severity in a large fire in a Pinuspinaster forest is highly predictable from burning conditions, stand structure, and topography. Ecosystems 18: 237-250. https://doi.org/10.1007/s10021-014-9824-y

Yebra M, Chuvieco E, 2009. Generation of a species-specific look-up table for fuel moisture content assessment. IEEE J Selected topics in applied earth observation and RS 2 (1): 21-26.

White JC, Wulder MA, Varhola A, Vastaranta M, Coops NC, Cook BD, Pitt D, Woods M, 2013. A best practices guide for generating forest inventory attributes from airborne laser scanning data using an area-based approach. Natural Resources Canada, Canadian Forest Service, Canadian Wood Fibre Centre, Victoria, BC. Information Report FI-X-010, 39 pp.

White JC, Wulder MA, Hobart GW, Luther JE, Hermosilla T, Griffiths P, Coops NC, Hall RJ, Hostert P, Dyk A, Guindon L, 2014. Pixel-based image compositing for large-area dense time series applications and science. Can J Remote Sens 40 (3): 192-212. https://doi.org/10.1080/07038992.2014.945827

White JC, Coops NC, Wulder MA, Vastaranta M, Hilker T, Tompalski P, 2016. Remote sensing technologies for enhancing forest inventories: a review. Can J Remote Sens 42: 619-641. https://doi.org/10.1080/07038992.2016.1207484

White JC, Wulder MA, Hermosilla T, Coops NC, Hobart GW, 2017. A nationwide characterization of 25 years of forest disturbance and recovery for Canada using Landsat time series. Remote Sens Environ 194: 303-321. https://doi.org/10.1016/j.rse.2017.03.035

Wulder MA, 1998. Optical remote-sensing techniques for the assessment of forest inventory and biophysical parameters. Progr Phys Geog 22 (4): 449-476. https://doi.org/10.1177/030913339802200402

Wulder MA, Dymond CC, 2004. Remote sensing in survey of Mountain Pine impacts: review and recommendations. MPBI Report. Canadian Forest Service. Natural Resources Canada, Victoria, BC, Canada. 89 pp.

Wulder MA, Masek JG, Cohen WB, Loveland TR, Woodcock CE, 2012. Opening the archive: how free data has enabled the science and monitoring promise of Landsat. Remote Sens Environ 122: 2-10. https://doi.org/10.1016/j.rse.2012.01.010

Wulder MA, Hilker T, White JC, Coops NC, Masek JG, Pflugmacher D, Crevier Y, 2015. Virtual constellations for global terrestrial monitoring. Remote Sens Environ 170: 62-76. https://doi.org/10.1016/j.rse.2015.09.001

Wulder MA, White JC, Loveland TR, Woodcock CE, Belward AS, Cohen WB, Fosnight EA, Shaw J, Masek JG, Roy DP, 2016. The global Landsat archive: Status, consolidation, and direction. Remote Sens Environ 185: 271-283. https://doi.org/10.1016/j.rse.2015.11.032

Xie Q, Zhu J, Wang Ch, Fu H, López-Sánchez JM, Ballester-Berman JD, 2017. A modified dual-baseline PolInSAR method for forest height estimation. Remote Sens-Basel 9 (8): 819. https://doi.org/10.3390/rs9080819

Xie Y, Sha Z, Yu M, 2008. Remote sensing imagery in vegetation mapping: a review. J Plant Ecol 1 (1): 9-23. https://doi.org/10.1093/jpe/rtm005

Zald HSJ, Wulder MA, White JC, Hilker T, Hermosilla T, Hobart GW, Coops NC, 2016. Integrating Landsat pixel composites and change metrics with LiDAR plots to predictively map forest structure and aboveground biomass in Saskatchewan, Canada. Remote Sens Environ 176: 188-201. https://doi.org/10.1016/j.rse.2016.01.015

Zarco-Tejada PJ, Diaz-Varela R, Angileri V, Loudjani P, 2014. Tree height quantification using very high resolution imagery acquired from an unmanned aerial vehicle (UAV) and automatic 3D photo-reconstruction methods. Eur J Agron 55: 89-99. https://doi.org/10.1016/j.eja.2014.01.004

Zarco-Tejada PJ, Hornero A, Hernández-Clemente R, Beck PSA, 2018. Understanding the temporal dimension of the red-edge spectral region for forest decline detection using high-resolution hyperspectral and Sentinel-2A imagery. ISPRS J Photogramm 137: 134-148. https://doi.org/10.1016/j.isprsjprs.2018.01.017